HHS Public Access

Author manuscript

Neuroimage. Author manuscript; available in PMC 2025 June 01.

Published in final edited form as:

Neuroimage. 2025 June ; 313: 121238. doi:10.1016/j.neuroimage.2025.121238.

Characterizing the effects of age, puberty, and sex on variability in resting-state functional connectivity in late childhood and early adolescence

Kelly A. Duffy[a,*], **Andrea Wiglesworth**[a], **Donovan J. Roediger**[b], **Ellery Island**[c], **Bryon A. Mueller**[b], **Monica Luciana**[a], **Bonnie Klimes-Dougan**[a], **Kathryn R. Cullen**[b], **Mark B. Fiecas**[c]

[a]Department of Psychology, University of Minnesota, Elliott Hall, 75 East River Parkway, Minneapolis, MN 55455, USA

[b]Department of Psychiatry and Behavioral Sciences, University of Minnesota, F282/2A West Building, 2450 Riverside Avenue South, Minneapolis, MN 55454, USA

[c]Division of Biostatistics, University of Minnesota, 2221 University Ave SE, Suite 200, Minneapolis, MN 55414, USA

Abstract

Understanding the relative influences of age, pubertal development, and sex assigned at birth on brain development is a key priority of developmental neuroscience given the complex interplay of these factors in the onset of psychopathology. Previous research has investigated how these factors relate to static (time-averaged) functional connectivity (FC), but little is known about their relationship with dynamic (time-varying) FC. The present study aimed to investigate the unique and overlapping roles of these factors on dynamic FC in children aged approximately 9 to 14 in the ABCD Study using a sample of 5122 low-motion resting-state scans (from 4136 unique participants). Time-varying correlations in the frontolimbic, default mode, and dorsal and ventral corticostriatal networks, estimated using the Dynamic Conditional Correlations (DCC) method, were used to calculate variability of within- and between-network connectivity and of graph theoretical measures of segregation and integration. We found decreased variability in global efficiency across the age range, and increased variability within the frontolimbic network driven primarily by those assigned female at birth (AFAB). AFAB youth specifically also showed

[*]Corresponding author. duffy379@umn.edu (K.A. Duffy).

CRediT authorship contribution statement

Kelly A. Duffy: Writing – review & editing, Writing – original draft, Visualization, Software, Methodology, Formal analysis, Data curation, Conceptualization. **Andrea Wiglesworth:** Writing – review & editing, Data curation, Conceptualization. **Donovan J. Roediger:** Writing – review & editing, Software, Methodology, Conceptualization. **Ellery Island:** Writing – review & editing, Data curation. **Bryon A. Mueller:** Writing – review & editing, Funding acquisition, Data curation, Conceptualization. **Monica Luciana:** Writing – review & editing, Supervision, Project administration, Funding acquisition, Conceptualization. **Bonnie Klimes-Dougan:** Writing – review & editing, Supervision, Funding acquisition, Conceptualization. **Kathryn R. Cullen:** Writing – review & editing, Supervision, Project administration, Funding acquisition, Conceptualization. **Mark B. Fiecas:** Writing – review & editing, Supervision, Methodology, Formal analysis, Conceptualization.

Declaration of competing interest

All authors declare no competing or conflicting interests.

Supplementary materials

Supplementary material associated with this article can be found, in the online version, at doi:10.1016/j.neuroimage.2025.121238.

increased variability in several other networks. Controlling for age, both advanced pubertal development and being AFAB were associated with decreased variability in all within- and between-network correlations and increased variability in measures of network segregation. These results potentially suggest advanced brain maturation in AFAB youth, particularly in key networks related to psychopathology, and lay the foundation for future investigations of dynamic FC.

Keywords

Dynamic functional connectivity; ABCD Study; Developmental neuroscience; Puberty; Sex differences; Dynamic conditional correlations

1. Introduction

Characterizing and understanding the development of the brain during childhood and adolescence has long been a priority of developmental neuroscience. Building on existing knowledge about the structural and functional changes that occur in the years prior to adulthood (Rashid et al., 2018; Wierenga et al., 2014) and given the critical role of adolescence in the development of psychopathology (Cicchetti and Toth, 2006; 2009; Luciana, 2013; Paus et al., 2008), important challenges ahead for the field include elucidating the exact roles of age and pubertal development in the typical maturational process. Understanding whether this process differs by sex assigned at birth, given the discrepancies in diagnosed mental health disorders by sex in this age range (Hayward and Sanborn, 2002) and differential risk for various types of mental health disorders (Christiansen et al., 2022), is crucial. However, this task is also complicated by the earlier onset of puberty (Patton and Viner, 2007) among female youth, which is itself linked to the development of psychopathology (Angold and Costello, 2006; Hayward and Sanborn, 2002). Given that a complex interplay of age, sex assigned at birth, and pubertal development has been linked to changes in the brain and the development of psychopathology in past work (López-Ojeda and Hurley, 2021; Wiglesworth et al., 2023), disentangling the unique and overlapping roles of these factors in the adolescent brain is essential for understanding clinically-relevant developmental processes.

Resting-state functional magnetic resonance imaging (rs-fMRI) can be used to characterize brain networks. Many research studies use fMRI data to measure resting-state functional connectivity (rs-FC; the correlation between signals from different regions of the brain) to understand large-scale neural networks and alterations in within- and between-network patterns of connectivity (e.g., Solé-Padullés et al., 2016). These rs-FC studies have fairly consistently identified age-related changes across childhood to young adulthood. One approach that has been used to characterize changes in functional connectivity is graph theory (Bullmore and Bassett, 2011; Rubinov and Sporns, 2010), where topological characteristics of brain networks are evaluated by considering brain regions as nodes in an overall network (graph). Graph theoretical approaches have identified increasing network segregation and definition from childhood into young adulthood, using metrics such as clustering coefficient, modularity, and local efficiency (Yu et al., 2018), as well as increased functional integration of networks (Fair et al., 2007) as young people mature. Research using

graph theoretical approaches has also identified sex differences in early adulthood, including that brain networks in young adult males generally have higher indicators of functional segregation while young adult females have higher indicators of functional integration of brain networks (Zhang et al., 2016). Sex differences in FC more broadly, including differing connectivity between particular networks (De Lacy et al., 2019) and higher overall FC values among males (Zhang et al., 2016), have also been identified in young adults. In adolescents and especially children, fewer consistent sex differences have been identified, but regional differences in FC (e.g., increased or decreased average rs-FC in one group relative to the other) have been found, such as in the precuneus (Solé-Padullés et al., 2016) and amygdala (Alarcon et al., 2015´). Additionally, some studies have found increased functional segregation and specialization of networks in female children and increased integration and global processing in male children (Wu et al., 2013), which is opposite to the pattern identified in young adults (Zhang et al., 2016).

The fewer sex-related findings in children and adolescents relative to young adults, and their inconsistency, have led to the suggestion (e.g., Sole-Padulles et al., 2016) that at least some sex differences may emerge as a result of pubertal changes, a proposition supported by a large body of past work. In particular, work in animal models has demonstrated that pubertal hormones (i.e., testosterone and estradiol) have an organizing effect on the brain during adolescence (Schulz et al., 2009; Schulz and Sisk, 2006), and further that the effect of these hormones on the brain and subsequent behavior are sex-dependent (Schulz and Sisk, 2016). Investigations into the effects of puberty and pubertal hormones on the brain in humans, and adolescents in particular, are more limited, but Herting et al. (2014) and Goddings et al. (2014) directly linked changes in pubertal hormone concentration and pubertal staging, respectively, to changes in brain volume. Gur & Gur (2016) also reported pre- and post-pubertal differences in brain structure, which are sex-specific. Studies directly investigating the effect of pubertal hormones on FC in particular are more limited, but a handful of studies have related pubertal staging to alterations in FC between specific regions during social and emotional processing in girls (Klapwijk et al., 2013) and testosterone levels to amygdala-OFC connectivity (Peters et al., 2015; Spielberg et al., 2015). Several more recent studies have investigated the effect of pubertal development more broadly on FC, and have found decreased cortical-subcortical FC (Van Duijvenvoorde et al., 2019) and increased functional segregation and efficiency as measured via graph theoretical approaches (Gracia-Tabuenca et al., 2021). Despite currently limited investigation into and evidence for the underlying hormonal mechanisms, several of these studies suggest that the developmental changes in FC fit better with models for pubertal development than for age (Gracia-Tabuenca et al., 2021; Van Duijvenvoorde et al., 2019), separately for both females and males (Van Duijvenvoorde et al., 2019), and that many of these metrics show a distinct inflection point around the onset of puberty (Gracia-Tabuenca et al., 2021).

The studies noted above have provided a critical foundation for understanding changes in the developing brain related to age, sex assigned at birth, and puberty. However, all used a traditional, “static” analysis of the rs-fMRI data that calculates the average FC over the entire course of the scan (“static connectivity”). These analyses may only provide one window into how the brain is functioning and organizing, and in particular may be limited because the approach inherently assumes that the overall functional network state, and its

key properties and connections, remain constant over the course of a resting-state scan. In fact, an increasing body of literature emphasizes the dynamic nature of brain states, even within resting state intervals (Chang and Glover, 2010), and recent work has begun to focus more on the dynamics of the correlated activity between regions over time as a way to further our understanding of brain function and organization. Analyses that investigate the time-related dynamics or the variability of FC over the course of the scan, known as "dynamic" analyses, may provide a unique vantage point into how the brain is able to dynamically and flexibly adapt to different situational and cognitive demands, and how the various subnetworks in the brain interact with each other over time. There are several different ways that dynamic FC can be evaluated, including through the variability of some metric (most often the correlation coefficient) calculated between individual brain regions or larger-scale networks across the course of the scan, through using clustering techniques to identify distinct "brain states" that individuals enter and spend varying amounts of time in across the course of the scan, and through time-varying measures of graph theoretical quantities that aim to summarize brain function; see Calhoun et al. (2014) and Hutchison et al. (2013) for a review. Metrics of dynamic connectivity have been shown to be related to various behaviors and cognitive abilities, including stimulus-related tasks, working-memory tasks, and overall cognitive performance (Cohen, 2018). Importantly, alterations in dynamic FC have been linked to several forms of psychopathology, such as schizophrenia, bipolar disorder, and depression (Calhoun et al., 2014; Hutchison et al., 2013), and in some instances these differences were obscured when evaluating only static FC (Damaraju et al., 2014), emphasizing the importance of incorporating dynamic measures.

Investigations into age-related changes in dynamic FC have found that temporal variability in the correlation between inherent functional networks increases from childhood to adulthood (Hutchison and Morton, 2015; López-Vicente et al., 2021; Qin et al., 2015), particularly in the between-network correlations involving core cognitive networks, such as the frontoparietal, default mode, and salience networks (Marusak et al., 2017). From the alternative, but potentially complementary, perspective of identifying brain states from clustering techniques, the specific types of brain states that individuals spend time in have also been shown to change across age, such that older individuals spend more time in more highly modularized and network-defined states (López-Vicente et al., 2021; Rashid et al., 2018). In addition, older individuals spend more time in particular in states with high connectivity within the default mode network (DMN), while younger individuals spend more time in states with high connectivity between the DMN and task-related networks like the cognitive control network (Faghiri et al., 2018) and more time in a more globally disconnected state (López-Vicente et al., 2021; Rashid et al., 2018). Developmental differences in dynamic connectivity related to sex assigned at birth are somewhat understudied, particularly from the perspective of the variability of FC, but recent work has found that children aged 10 to 14 who were assigned female at birth (AFAB) had a broadly more mature pattern of dynamic connectivity than those assigned male at birth (AMAB), spending more time in more highly modularized and distinguished states (López-Vicente et al., 2021). In young adults, past work has found that those AFAB spend more time in segregated brain states with high within-network connectivity, particularly between subnetworks of the DMN, while those AMAB have higher connectivity between

certain task-related and sensory networks and generally display greater fluidity in shifting dynamically between states (De Lacy et al., 2019). Whether these differences based on sex, particularly those that show a relatively faster development of dynamic connectivity and emergence of a more mature connectivity pattern among those AFAB or females (López-Vicente et al., 2021; Satterthwaite et al., 2015), are related to pubertal development is unknown, as there are at present no direct investigations into the effect of pubertal development on FC using dynamic analyses.

The present study aims to build and expand upon the previous work investigating the dynamic patterns of rs-FC in children and adolescents. In particular, we hope to provide additional insight into the somewhat limited and sometimes conflicted investigations into how dynamics change as children age and undergo pubertal development, as well as how connectivity patterns may differ based on sex assigned at birth. To evaluate brain dynamics, we will specifically focus on measuring the temporal variability of the correlation within- and between certain networks of interest: the frontolimbic network, the default mode network, and the dorsal and ventral corticostriatal networks. These networks were chosen due to identified alterations in these networks during development in previous research (De Lacy et al., 2019; Faghiri et al., 2018; Marusak et al., 2017) and because of their implications in the development of psychopathology (Furman et al., 2011; Harrison et al., 2009; Kebets et al., 2021; Whitfield-Gabrieli and Ford, 2012; Zhong et al., 2016). We will also evaluate dynamic FC by measuring the temporal variability of several graph metrics that summarize overall network segregation (measured using local efficiency, clustering coefficient, and transitivity) and integration (measured using global efficiency) across the course of the scan. In doing so, we aim to complement the results of the within- and between-network variability by more directly evaluating the functional configuration of these networks. We also aim to fill a gap in the literature by simultaneously investigating how these measures, network variability and graph metric variability, relate to both developmental changes and to each other.

To investigate the relationship between dynamic FC and age, sex assigned at birth, and pubertal development, we leverage two early data points (during late childhood and early adolescence) from the large-scale, longitudinal Adolescent Brain Cognitive Development (ABCD) Study, which utilized a population-based approach to enroll over 11 thousand children ages 9 and 10 years and is currently following them longitudinally over ten years. We use the Dynamic Conditional Correlations (DCC; Lindquist et al., 2014) method to construct correlation matrices over time across a low-motion resting state scan. These correlation matrices are then used to determine the variability of the correlations between nodes (i.e., brain regions) in the networks of interest and of the graph metrics calculated from the matrices across time. Overall, we consider fifteen outcomes related to dynamic FC: the variability of four graph metrics (global efficiency, local efficiency, clustering coefficient, and transitivity), the within- and between-network variability of four networks (frontolimbic network, default mode, and dorsal and ventral corticostriatal), and overall average FC variability in the four networks across the course of the scan. The first aim is to evaluate how these outcomes differ as a function of age, and whether the effect of age differs based on sex assigned at birth. The second aim is to evaluate how these outcomes differ as a function of pubertal development (controlling for age), and whether the effect

of pubertal status interacts with sex assigned at birth. The third aim is to investigate how these outcomes differ by sex assigned at birth across all ages and pubertal stages. As the literature investigating the relationships between dynamic FC and age, sex assigned at birth, and pubertal development is somewhat limited, particularly from the dynamic perspective of evaluating variability rather than brain state transitions, we had limited prior hypotheses and aimed for the current study to be exploratory in nature. However, we did expect to replicate certain previous findings from the literature, such as increased variability within- and between certain networks as children mature (Hutchison and Morton, 2015; López-Vicente et al., 2021; Marusak et al., 2017; Qin et al., 2015), more mature brain patterns in AFAB youth (López-Vicente et al., 2021; Rashid et al., 2018; Satterthwaite et al., 2015), and changes in the overall segregation and integration properties of the underlying functional network state across development (López-Vicente et al., 2021; Rashid et al., 2018).

2. Materials and methods

2.1. Sample

The sample consisted of participants from the ABCD Study (Volkow et al., 2018), a 21-site longitudinal study tracking demographic, physical, psychological, environmental, and other variables from a large cohort of children across time. The ABCD study consists of a sample of 11,878 participants that were recruited at ages 9–10 for the initial ("baseline") data collection using a sampling strategy that aimed to recruit an epidemiologically-informative sample reflective of the sociodemographic variation in the United States (Garavan et al., 2018). Note that the ABCD Study was designed explicitly with the aim of following participants longitudinally into young adulthood. Each ABCD data collection site obtained institutional review board (IRB) approval either locally or from a central IRB at the University of California San Diego (Auchter et al., 2018). From this initial sample, data from individual participants was included here if they had resting state fMRI data of sufficient quality (i.e., meeting inclusion criteria, see "Imaging Data Acquisition and Preprocessing" for further information) at either baseline data collection ("Baseline"), the year 2 follow up event ("Year 2"), or both. This resulted in 5122 total observations (at either Baseline or Year 2) from 4136 unique participants. Data at Baseline consisted of 2594 participants, while data at Year 2 consisted of 2528 participants. The demographic information for the overall sample (including both time points), as well as the demographic characteristics of the unique samples at Baseline and Year 2, are presented in Table 1.

2.2. Measuring age, sex assigned at birth, and pubertal status

Sex assigned at birth was measured using parental (or primary caregiver) report. Specifically, parents were asked what sex the child was assigned at birth on their original birth certificate, with response options of "Male," "Female," "Intersex-Male," "Intersex-Female," "Don't Know," or "Refuse to Answer." In the sample used within the present study (a sub-sample of all ABCD participants), no parents endorsed the "Intersex-Male" or "Intersex-Female" option for their children. Note that throughout the rest of the manuscript, for simplicity and readability, we will be referring to our measure of sex assigned at birth simply as "sex," but continuing to use assigned male at birth (AMAB) and assigned

female at birth (AFAB) to emphasize the distinction. Pubertal status was measured using the Pubertal Development Scale (PDS; Petersen et al., 1988), a completely text-based (i.e., involving no physical examination or measures) assessment of perceived pubertal development. Both youth and parents complete the PDS in ABCD, but here we elected to focus on parent-report, as is suggested in the literature for ABCD data collected at baseline given the large proportion of "Don't Know" responses at this age range (Cheng et al., 2021). The PDS is based on five questions regarding developmental changes in height, body hair, and skin, as well as questions regarding voice and facial hair for males and breast development and menarche (which includes follow-up questions if reported) for females. Each question is rated on a four point scale, and summary scores were then created by the ABCD team, separately for those AMAB and AFAB, to classify individuals into five categories: pre-pubertal (1), early pubertal (2), midpubertal (3), late pubertal (4), postpubertal (5). The criteria for categorization was based on the totality of responses to particular items, which differed for those AMAB and AFAB, and is thoroughly outlined in Herting et al. (2021, p. 4). The PDS has been shown to correlate well with other measures of pubertal development, such as physician ratings (Petersen et al., 1988) and hormonal changes (Shirtcliff et al., 2009), including in ABCD (Herting et al., 2021). Age was measured in months based on the difference between the participant's date of birth and the date the participant began data collection for their ABCD study visit. Note that it is possible for different measures (e.g., interview-based measures, like the PDS, and MRI scanning) to occur on different days or visits, slightly changing the participants' exact age for the various measures, but this difference is generally extremely small and absorbed by rounding at the month level.

2.3. Imaging data acquisition and preprocessing

Resting state functional magnetic resonance imaging (rs-fMRI) data was collected at both Baseline and Year 2 data collection events at each study site in accordance with ABCD protocols. For further information on ABCD imaging acquisition parameters and scanning protocols, see Casey et al. (2018), and for further information on minimal preprocessing and quality control (QC) procedures, see Hagler et al. (2019). Briefly, resting-state imaging data were acquired at each study site and harmonized across the 3T scanning platforms (Siemens Prisma, Philips, GE 750). Several (typically four, but variable dependent on individual data collection circumstances and participant motion) five-minute (TR = 800 ms, 2.4 mm isotropic acquisition) resting-state runs were collected for each participant using multiband *EPI* with slice acceleration and fieldmap scans for distortion correction. All scans were verified for protocol compliance and initial QC by the ABCD Data Analysis and Informatics Center (DAIC). Data were then processed through a specialized ABCD-BIDS pipeline developed and implemented as part of the ABCD-BIDS Community MRI Collection (ABCC); for full details on this pipeline and the processing, see Feczko et al. (2021). Briefly, anatomical data are normalized, template-aligned, and converted into CIFTI format, and the co-registered resting-state volumetric fMRI data are brought into CIFTI space using normalization and projection onto the CIFTI format. These CIFTI data are then further processed using the Developmental Cognition and Neuroimaging (DCAN) Lab's BOLD preprocessing program (Fair et al., 2020), which includes a 2 mm FWHM Gaussian spatial filter. The minimally processed time courses then undergo nuisance regression based

only on low-motion frames (< 0.30 mm framewise displacement [FD]) after specialized respiratory motion filtering is applied (Fair et al., 2020), followed by temporal filtering (using a second-order Butterworth filter of 0.009–0.08 Hz). Note that prior to temporal filtering, linear interpolation is used to replace high motion frames (> 0.30 mm FD), such that only "good" data is used while also avoiding aliasing from missing time points. Following processing, parcellated time series are then constructed using a variety of atlases; the present analyses used the Human Connectome Project (HCP) 360 region of interest (ROI) atlas (Glasser et al., 2016).

Following processing, we selected individual runs of individual participants for use in subsequent analyses. Several aspects regarding the DCC approach informed data selection. First, although the DCAN Lab's BOLD preprocessing recommends censoring high-motion data frames, the DCC method relies on data from previous time points to inform estimation of the time-varying model parameters. Thus, the removal of time points disrupts the time series which impacts estimates of the autocorrelation structure and downstream analyses. For this reason, censoring data points is not recommended with this method (Lydon-Staley et al., 2019; Syed et al., 2017). Notably, however, the DCAN processing pipeline linearly interpolates time points that otherwise would be censored following filtering. The effect of this linear interpolation on the DCC method as applied to neuroimaging data is unknown, although despiking, a form of interpolation, has been shown to perform well in dynamic analyses broadly (Lydon-Staley et al., 2019). Linear interpolation has been deployed in other non-imaging uses of the DCC method to account for missing data (Chittedi, 2015; Zhang and Chan, 2009), and previous limited investigations, again in other contexts, suggest there may be a positive impact of interpolation (Barucci and Reno, 2002) and that bias is such that the estimated volatility of the time series is downwardly biased, which is less likely to lead to spurious findings. However, to avoid the potential risk that interpolation influences results, we aimed to keep interpolation to a minimum. Thus, selected data was limited to runs that had ten or fewer frames (out of 375 total frames, after removal of initial volumes for stabilization, for full-length runs) that were linearly interpolated (i.e., that were above 0.30 mm FD), meaning only extremely low-motion runs were included. For participants who had runs meeting this criteria, the lowest motion run (determined by a combination of the number of frames below threshold, mean FD, and maximum FD) for each individual was selected provided that the run was at least 350 frames. Data from participants that failed the ABCD team's overall resting-state QC measurements (Haist and Jernigan, n.d.; Hagler et al., 2019) were also excluded. Following these exclusion criteria, there were $n = 2594$ participants with data of sufficient quality at Baseline and $n = 2528$ at Year 2.[1]

2.4. Dynamic conditional correlations (DCC) analysis

The DCC method was applied to processed and parcellated time series so that dynamic FC could be assessed. The DCC method (Engle, 2002), with application to FC data introduced by Lindquist et al. (2014), is a type of multivariate generalized autoregressive conditional

[1]Note that, although the full ABCD sample is 11,878 participants, at the time of writing there were notably fewer participants (approximately 7,500 at Baseline and 5,500 at Year 2) that had data fully processed through the updated ABCD-HCP pipeline that we were able to access. This, combined with our strict motion criteria, led to the notably smaller than (theoretically) possible number of participants.

heteroscedastic (GARCH) model (Bollerslev, 1986). Broadly, the aim of the DCC approach is to estimate the conditional correlation between all ROIs at each time point using a weighted combination of previous estimates of the conditional correlation along with the current observations. Unlike a sliding window approach, which sets a fixed window length and equally (or through a set taper function) weights all time points, the window length in DCC is variable and determined using a quasi-maximum likelihood approach based on the prior behavior of the time series. DCC has been shown to have greater reliability than sliding window approaches in separating true time-varying FC changes from noise (Choe et al., 2017; Lindquist et al., 2014). DCC also circumvents several issues inherent to a sliding window approach, such as the need to determine the correct window length or degree of window overlap. See the Supplementary Materials for further mathematical details of the DCC method.

The DCC method was applied to construct one correlation matrix at each time point (i.e., each frame of the run), consisting of correlations between all 360 ROIs in the selected Glasser atlas for each individual's selected run. The first 5 matrices were then dropped from analyses, to allow the model to stabilize. To focus only on selected networks of substantive interest (i.e., those shown in past research to show strong developmental changes and to be related to psychopathology), only ROIs that were determined (as part of the current study, in consultation with the literature and the grouping of parcels/clusters described in the Supplementary Neuroanatomical Results of Glasser et al., 2016) to be part of the fronto-limbic network (consisting of regions in the ACC/mPFC, insula, amygdala, and hippocampus) (Craske et al., 2017; Williams, 2017), default mode network (consisting of regions in the ACC/mPFC, posterior cingulate, angular gyrus, and middle temporal region) (Raichle, 2015; Raichle et al., 2001), dorsal cortico-striatal network (consisting of regions in the dorsolateral PFC, dorsal ACC/mPFC, dorsal parietal cortex, caudate, and putamen) (Insel et al., 2017), ventral cortico-striatal network (consisting of regions in the ventral ACC/mPFC, orbitofrontal cortex, and accumbens) (Casey, 2015) were included. See Supplementary Materials for a list of all Glasser parcels used in analyses and further description. The Fisher-transformed correlations between this subset of ROIs was then used to calculate the subsequent metrics.

2.5. Network and graph metric variability calculation

The output from the DCC method was then used to calculate different metrics of variability. First, several different graph metrics were calculated using the series of correlation matrices, such that one graph per time point (using the selected ROIs, outlined above, as nodes) was constructed for each participant. Unweighted, directed graphs were constructed from the Fisher-transformed DCC correlation matrices, setting all negative weights to zero, and then Brain Connectivity Toolbox (Rubinov and Sporns, 2010) was used to calculate the graph metrics of interest. To evaluate integration between the subnetworks of interest, global efficiency was calculated for each individual at each included time point. Briefly, global efficiency is the inverse of the average shortest "path length" (number of links needed to connect two nodes, which here are parcels) in a network, and represents how efficiently information can transfer across an entire network (Latora and Marchiori, 2001; Rubinov and Sporns, 2010). To evaluate segregation within the subnetworks of interest, local efficiency,

clustering coefficient, and transitivity were calculated. Local efficiency is the inverse average shortest path length only among parcels directly connected to the parcel of interest, and represents how efficiently information can transfer within a local collection of nodes (Latora and Marchiori, 2001; Rubinov and Sporns, 2010). Clustering coefficient is, informally, the fraction of a node's (parcel's) connecting parcels that are also connected to each other, and thus reflects the average clustered connectivity around individual parcels (Rubinov and Sporns, 2010; Watts and Strogatz, 1998). Clustering coefficient is calculated by normalizing each parcel individually based on its own number of connections, and thus can be skewed by parcels with few connections. Transitivity is a variant of clustering coefficient that normalizes each parcel collectively based on the overall network, and thus is more robust to this issue (Newman, 2003; Rubinov and Sporns, 2010). For further mathematical details of these graph metrics, see the Supplementary Materials. For each individual, the overall variability of these graph metrics was then calculated using the standard deviation of the according metric across all of the included time points.

Next, within- and between-network variability across the scan was calculated for each individual. Four networks (fronto-limbic, default mode, dorsal cortico-striatal, and ventral cortico-striatal) were defined using parcels from the Glasser atlas, as briefly described above; see the Supplementary Material for further information on the parcels included in each network. For each network, within-network variability was calculated by taking the average of the pairwise (i.e., between each parcel included in the network) standard deviation values calculated across the time series. For each network pair, the between-network variability was calculated by taking the average of the pairwise standard deviation values calculated between each pair of parcels in the two according networks. Importantly, some of the parcels overlapped between networks, and were considered part of both networks by definition. In this case, their variability with each other corresponding parcel in the network was only considered once, to avoid counting these connections twice in the calculation of the overall mean. These individual-level within- and between-network measures of variability, as well as the graph metric variability, across the scan were then used in subsequent statistical analyses.

2.6. Statistical analyses

Following the calculation of graph metric variability and within- and between-network variability across the scan for each individual, statistical analyses were performed to evaluate the relationships between this variability and age, pubertal status, and sex within the sample. A series of generalized additive mixed effect (GAMM) models (Lin and Zhang, 1999) and linear mixed effects (LME) models (Laird and Ware, 1982), where appropriate, were carried out. GAMMs are an extension of generalized additive models (GAMs) that include random effects, which are used to address data where the assumption of independent observations is violated, such as with longitudinal data or data from related individuals. GAMs are nonparametric and have the advantage of not needing to assume any particular form of the relationship between variables (e.g., a linear relationship), but rather use smooth functions to estimate the form of the relationship based on the data (Hastie and Tibshirani, 1987). When predictors are only categorical in nature, however, no smooth relationship between the levels of the predictor and the outcome are possible, so we elected to use LMEs in this case.

Given that we are modeling longitudinal data, that includes repeated measures from some participants, and relationships between individuals in terms of both family and ABCD site effects, a mixed effects-type model (i.e., an LME or GAMM) incorporating random effects is appropriate.

To fit the series of models, we first used the four measures of graph metric variability (global efficiency, local efficiency, clustering coefficient, and transitivity) as outcomes in models using age (measured in months), sex (assigned at birth, measured dichotomously), and pubertal status (measured with 5 ordered levels) as separate main effects, as well as models looking at the interaction of sex with both age and pubertal status. Note that the interaction between sex and pubertal status is used to investigate whether the effect of pubertal development differs based on sex, although the distribution of PDS scores differs quite notably between those AMAB and AFAB (Table S6). Age (and its interaction with sex) was modeled using GAMMs, sex was modeled using LMEs, and pubertal status (and its interaction with sex) was modeled first using GAMMs (treating pubertal status continuously) and then confirmed using LMEs (treating pubertal status categorically). This process was then repeated using the 10 measures of within- and between-network variability in our four networks of interest (frontolimbic, default mode, dorsal and ventral corticostriatal) plus overall variability as outcomes. For GAMMs, (approximate) p-values were calculated using Wald-type tests against the null hypothesis that the overall smooth term is zero. These tests are based on the Bayesian confidence intervals for the smooth effects (Nychka, 1988), with the model degrees of freedom calculated based on the trace of (a function of) the hat matrix; see Wood, 2013 for more details. For LMEs, (approximate) p-values were calculated using the R package lmerTest (Kuznetsova et al., 2020). These p-values are based on F-tests where Satterthwaite's method is used to calculate the denominator degrees of freedom; see Kuznetsova et al., 2017 for more details. Within each model (e.g., looking only at the main effect of age on the variability of graph metrics), a Benjamini-Hochberg correction for multiple comparisons (Benjamini and Hochberg, 1995) was used to correct the resultant p-values of the relevant predictor on the total number of outcomes (either 4 or 11). All models included a set of demographic covariates (household income, highest parental education, parent-identified race and ethnicity of the child, parental marital status, and MRI scanner manufacturer; see Table 1 and the according notes for further details on the levels of these variables), and included random effects for individuals, families, and data collection site, to account for the longitudinal nature of the data and the nested data collection structure of ABCD (where individuals are nested both within families and within data collection sites). Models looking at the effect of age additionally included sex and pubertal status as covariates. Pubertal status and sex were highly related in the present sample due to the (expected) greatly increased pubertal maturity in those AFAB. As these effects were so closely related, models for pubertal status and sex (either as main effects or interaction models) were fit both with and without using the other as a covariate, but always included age as a covariate. All analyses were carried out using R (R Core Team, 2024), with GAMM models fit using the gamm4 package (Wood and Scheipl, 2020) and LME models fit using the lme4 package (Bates et al., 2024).

3. Results

Note that for all analyses, full results are available in the Supplementary Materials (Tables S2, S3, and S5). For age, sex, and age-by-sex analyses, all results that showed statistical significance are displayed in figures. Due to the large number of significant effects for the analyses involving pubertal status, a selection of illustrative findings are presented as figures, and a complete set of results can be found in the Supplementary Materials.

Age and graph network variability.

The variability of global efficiency across the scan was significantly related to age, while no other graph metrics showed significant effects in variability (Table S2, in Supplementary Material). Plotting the smooth effect of age (Fig. 1a), we found that age has a nonlinear negative relationship with the variability of global efficiency, where variability decreases as children age. When looking at the (significant) interaction between age and sex, we found that both AFAB and AMAB youth had significant relationships between age and the variability of global efficiency (Table S2), but of a slightly different nature. Plotting the smooth effect separated by sex (Fig. 1a), we found that those AFAB show a negative linear relationship between age and global efficiency variability across the entire age range under study (107 to 165 months), while those AMAB show no relationship until around 130 months, at which point variability in global efficiency begins to decline.

Age and the variability of within- and between-network connectivity.

Only within-frontolimbic network variability had a significant relationship with age (Table S2). Plotting the smooth effect of age (Fig. 1b), we find that within-frontolimbic variability shows a positive linear relationship with age, such that older children have more variability within this network. When looking at the interaction between age and sex, we find that only those AFAB have a significant relationship between age and variability (Table S2) and appear to be driving the overall effect. Those AFAB also show significant or borderline significant (note that since these p-values are approximate, we also evaluated the effect of interest for the several terms that were just above an FDR-corrected p-value of 0.05) relationships between age and within-default mode network variability, as well as variability between the frontolimbic and ventral cortico-striatal networks, the frontolimbic and dorsal cortico-striatal networks, the frontolimbic and default model networks, and the default mode and ventral corticostriatal networks, and in overall variability across all nodes (mean SD). Those AMAB show no significant relationships between age and within- or between-network variability (Table S2). Plotting the smooth effects (Fig. 1b and Figure S5 [Supplementary Materials]), we can see that those AMAB show a slight linear decline in the variability of all within- and between-network correlations except for within-frontolimbic connectivity, which shows a slight linear increase. Those AFAB, on the other hand, generally have more nonlinear effects, with the exception of the variability between the default mode and ventral corticostriatal networks, which shows a linear increase. For all other network correlations, as well as variability in overall mean connectivity, those AFAB have a plateau or slight decline from the youngest age (around 110 months) until around 125 months, where variability increases until around 145 months, and then again plateaus or slightly declines (with much less certainty in the direction of the effect at higher ages).

Notably, the variability of within-frontolimbic connectivity shows the sharpest increase over this time period for those AFAB, and again suggests that those AFAB are driving the overall age effect (although those AMAB also show a slight linear increase with age).

Pubertal status and graph network variability.

The variability of global efficiency, local efficiency, clustering coefficient, and transitivity all show significant relationships with pubertal status when pubertal status is treated continuously (Table S3). As noted in the Methods section, however, given that pubertal status is an ordinal variable, we also performed a LME treating pubertal status categorically. These results (presented in the Supplementary Materials, Table S4) show that the variability of GE is only significant (relative to Pre-Puberty, PDS category 1) in the Mid-Puberty (PDS category 3) and Post-Puberty (PDS category 5) groups, while all other metrics show significant differences in all categories. Thus, we find that the variability of local efficiency, clustering coefficient, and transitivity do indeed show a significant relationship with pubertal status, but conclude that the variability of global efficiency only shows a strong, reliable relationship with age. Looking at the smooth effects (Fig. 2a), we can see that transitivity shows a strong linear relationship with pubertal status, such that those at a higher pubertal status show more variability in transitivity. The relationships between the variability of local efficiency and clustering coefficient with pubertal status are nonlinear, with both showing an increase from Pre-Puberty (PDS category 1) to Early Puberty (PDS category 2), somewhat of a plateau between Early Puberty and Mid-Puberty (PDS categories 2 and 3), and then a sharp increase from Mid-Puberty to Post-Puberty (PDS categories 3 through 5). Although the confidence bands around the Late Puberty (PDS category 4) and, in particular, Post-Puberty (PDS category 5) are wide, due to the smaller number of individuals in these groups, and warrant some skepticism, we again highlight that the categorical results in the Supplementary Materials show a significant difference for each PDS category relative to Pre-Puberty for these metrics, and thus there does appear to be a significant effect of pubertal status. When further controlling for sex, in addition to age and the set of demographic covariates, all effects became non-significant. There were no significant interactions between pubertal status and sex.

Pubertal status and the variability of within- and between-network connectivity.

A significant relationship was found between pubertal status and the variability of all within- and between-network correlations, as well as overall variability of the mean connectivity across all nodes (Mean SD) when treating pubertal status continuously (Table S3). Looking at the smooth effects (Fig. 2b and Figure S6 [Supplementary Materials]), we can see that for every within- and between-network correlation, except within the dorsal corticostriatal network, there is a linear decline in variability as pubertal status increases. In other words, stability in these networks increased with pubertal maturation. Within the dorsal corticostriatal network, there is a slight linear decrease between Pre-Puberty and Late Puberty (PDS categories 1 through 4) followed by a sharp decline between Late Puberty and Post-Puberty (PDS categories 4 and 5) (with the caveat again that results for the Post-Puberty group, with a small number of individuals, should be evaluated with caution). Results treating the PDS groups categorically (presented in the Supplementary Materials) confirm these results, and find that relative to Pre-Puberty (PDS category 1), all within- and

between-network correlations show a significant difference in variability between all PDS categories, with the exception of four networks (within the ventral corticostriatal network, within the dorsal corticostriatal network, between the dorsal and ventral corticostriatal networks, and between the default mode and dorsal corticostriatal networks) where differences were not significant (ps < 0.11) for Early Puberty (PDS category 2) relative to Pre-Puberty (PDS category 1), but were significant for all other categories. When further controlling for sex, in addition to age and the set of demographic covariates, all effects became non-significant. There were no significant interactions between pubertal status and sex.

Sex assigned at birth and graph theory metrics.

We found a significant relationship for the variability of all graph metrics considered (global efficiency, local efficiency, clustering coefficient, and transitivity) with sex (Table S5). Looking at the direction of the effect (Table S5, Fig. 3), we found that those AFAB have higher variability in all metrics than those AMAB. These effects remained significant when controlling for pubertal status in addition to age and the demographic covariates, and Fig. 3 shows the effect controlling for pubertal status.

Sex assigned at birth and the variability of within- and between-network connectivity.

We found a significant relationship for the variability of all within- and between-network correlations, as well as overall variability of the mean connectivity across all nodes (mean SD) (Table S5) with sex. Looking at the direction of these effects (Table S5, Fig. 3), we found that those AFAB had lower variability, relative to those AMAB, for all within- and between-network pairs. These effects remained significant when controlling for pubertal status in addition to age and the demographic covariates, and Fig. 3 shows the effect controlling for pubertal status. There were no significant interactions between sex and pubertal status for either graph metric variability or within- and between-network variability.

4. Discussion

The goal of the present study was to investigate the unique and overlapping roles of age, sex, and pubertal development on adolescent dynamic rs-FC in a large, population-based sample to better understand and characterize developmental changes in FC patterns. Unlike static FC analyses, which average connectivity values across the course of a scan, dynamic FC analyses enable investigating the variable organization of neural activity across the course of a scan. These dynamic patterns may hold particular relevance for behavioral and cognitive measures (Cohen, 2018) and may even potentially serve as biomarkers for psychiatric diagnoses (Damaraju et al., 2014; Hutchison et al., 2013). Establishing a baseline of developmental changes in dynamic FC is thus essential, but the effects of maturation related to both age and pubertal development, as well as how these may differ due to sex, is relatively understudied. We aimed to add to this literature by investigating dynamic FC in children and adolescents, where dynamic FC was operationalized as the variability of within- and between-network correlations and the variability of graph metrics across the course of a resting state scan. We focused analyses on a subset of networks, the frontolimbic, default mode, and dorsal and ventral corticostriatal networks, identified previously in the

literature to be related to both development (Faghiri et al., 2018; Marusak et al., 2017) and psychopathology (Furman et al., 2011; Harrison et al., 2009; Kebets et al., 2021; Whitfield-Gabrieli and Ford, 2012; Zhong et al., 2016). To construct the variability measures, of both the network correlations and the graph metrics, we used the DCC method (Lindquist et al., 2014), which has been shown to have greater reliability in separating signal from noise than alternative sliding window techniques (A.S. Choe et al., 2017), using a sample of 5122 resting state scans that met strict low-motion criteria from 4136 unique children aged approximately 9 to 14 years who participated in the ABCD Study.

The first aim was to explore how the different outcomes (variability of graph metrics and variability of within- and between-network correlations) differ as a function of age, and whether this age effect differs based on sex. We found that the variability of global efficiency, a measure of overall network integration, significantly declined across the age span, and that the pattern was slightly different for youth AFAB and AMAB. Youth AFAB demonstrated a sustained decline across the entire age range under study, while those AMAB did not show a decline until around 130 months of age (~10.8 years). This suggests that as children age, they are spending more time in more stable network states (at least between the networks under study) in terms of overall network integration. This supports previous findings that as children age, they spend less time in a globally disconnected state and more time in more modularized states (López-Vicente et al., 2021; Rashid et al., 2018), and that increased integration of functional networks is a key characteristic of the developing brain (Fair et al., 2007). The present results also suggest that this transition may be occurring earlier in those AFAB relative to those AMAB.

For within- and between-network variability, we found that connectivity within frontolimbic regions was characterized by increased variability across the age span, and that this effect was driven largely by youth AFAB, as those AMAB showed a much weaker relationship. We also found that those AFAB showed generally positive (but typically nonlinear) relationships between age and mean overall network variability, as well as variability within the default mode network, between the frontolimbic and default mode networks, between the frontolimbic and dorsal and ventral corticostriatal networks, and between the default mode and ventral corticostriatal networks. All of these within- and between-network correlations, as well as mean connectivity, showed a particularly sharp increase in variability between ages 125 and 145 months in youth AFAB. Those AMAB generally showed a weak decline in the variability of these same network pairs across the age range. Past work has demonstrated increased temporal variability between networks as individuals get older (López-Vicente et al., 2021; Marusak et al., 2017; Qin et al., 2015), particularly between core cognitive networks such as the frontoparietal, default mode, and salience networks (Marusak et al., 2017). These results suggest that, at least in this particular age range, these increases in variability may be strongest within the frontolimbic network, and that age-related increases in connectivity between other networks may be seen sooner in those AFAB than those AMAB. Given the implications of the variability of frontolimbic network connectivity in emotional dysregulation across multiple psychiatric diagnoses (Kebets et al., 2021), and the broader implications of the frontolimbic network in depression (Zhong et al., 2016) as well as other clinical conditions, this finding may have clinical relevance. In particular, how or whether this finding may relate to the increased risk for youth

AFAB, relative to AMAB, to experience clinically elevated levels of depression across the adolescent period (Hayward and Sanborn, 2002; Kessler et al., 2005), remains an important open question for future research.

The second aim was to investigate how variability changes as a function of pubertal development. We found, controlling for age, that the variability of clustering coefficient, transitivity, and local efficiency, all measures of network segregation, increased along with pubertal development. We found that all within- and between-network correlations, as well as overall average connectivity, decreased in variability as pubertal development progressed, controlling for age. The graph metric results are supported by previous static connectivity literature which found that measures of segregation and local efficiency across the brain increased beginning around the onset of puberty (Gracia-Tabuenca et al., 2021), and previous work generally supports the strengthening of distinct functional networks across pubertal development (Van Duijvenvoorde et al., 2019). Although the link between the magnitude of graph metrics and the variability of these metrics is not well-understood, we can speculate on their relationship and how to interpret the present findings. Speculatively, the increased variability in graph metrics relating to network segregation may suggest that those with a more advanced pubertal status are fluctuating more either into, or between, distinct, modularized brain networks, rather than spending time in more diffuse, generalized network states, which may be harder to identify as distinct network states and thus would register as less variability due to more time in these (potentially fewer) diffuse states. This pattern, spending more time in more defined (i.e., less diffuse) states, is seen in more mature brains (López-Vicente et al., 2021; Rashid et al., 2018). Spending more time in more functionally distinct and modularized network states may also explain the decreased variability in all within- and between-network correlations, as these network configurations, which are functionally defined, may be more stably reflected in those with a more advanced pubertal status. Importantly, these networks are also defined on more mature adult brains, and the decreased variability of those with a more advanced pubertal maturity may reflect better coherence with the functional network definitions.

Notably, however, when controlling for sex in addition to age, none of the effects of pubertal status retained their statistical significance. This is likely due to the large discrepancy in PDS (the measure used to evaluate pubertal status) scores between those AFAB and AMAB in this sample: nearly all individuals considered Late Puberty (PDS score of 4) were AFAB, and virtually all individuals considered Post-Puberty (a PDS score of 5) were AFAB (see Supplementary Materials, Table S6). This trend of more advanced pubertal development in those AFAB is expected in this age range and is commonly reported in the literature (Patton and Viner, 2007; Thijssen et al., 2020; Wiglesworth et al., 2023). Due to the lack of those AMAB participants characterized by later pubertal stages and the relatively more advanced pubertal development in AMAB, disentangling the effects of pubertal status and sex is extremely difficult in the present study. This may also serve to explain why the interaction effects between pubertal status and sex were not significant for any of the analyses. Due to the differences in the PDS distributions, we may have been unable to detect group-specific differences due to somewhat limited power, particularly if group differences are primarily in the upper ranges of the PDS scale, which is largely unobserved in the sub-sample AMAB. Future work analyzing a wider range of PDS scores across sex, which will necessitate

a more maturationally developed sample than is currently available in the ABCD Study time points with imaging data, should serve to shed more light on differential maturational patterns. In particular, matching individuals AFAB and AMAB based on age in a limited (older) range where there is greater variability in PDS scores should help to disentangle effects, and allow for a more direct investigation of sex differences in pubertal effects. As additional longitudinal data become available within ABCD, this question can be pursued through additional research. At present, we were limited by the availability of imaging data processed in the format necessary for the DCC analyses. Pubertal status information has already been collected for subsequent years of the ABCD Study, and as such, future research will be able to investigate this using pretabulated fMRI data or upon the release of additional ABCC-processed fMRI data.

The third aim was to investigate how variability differed based on sex assigned at birth. We found that, controlling for the effects of both age and pubertal status, youth AFAB had significantly higher variability in all graph metrics considered: global efficiency, local efficiency, clustering coefficient, and transitivity. We also found that those AFAB had decreased variability in all within- and between-network correlations, as well as decreased variability in overall mean connectivity, relative to those AMAB. Notably, these results are very similar to the results looking at the effect of pubertal status, with the direction of the effects for those AFAB being the same as those with a more advanced pubertal status. Although the results for sex did account for pubertal status, as mentioned above, the AFAB group is far more pubertally advanced than the AMAB group, and as such, disentangling the effects of pubertal status and sex is difficult in the present study. The results for sex may indeed reflect advanced brain maturation among those AFAB, a phenomenon widely observed in the literature (López-Vicente et al., 2021; Rashid et al., 2018; Satterthwaite et al., 2015). This phenomenon is often attributed to advanced pubertal development among those AFAB (López-Vicente et al., 2021), and indeed we see an uneven distribution of PDS scores between those AFAB and AMAB that may be driving this result, but it is also possible that differences in sex precede pubertal development. However, these nuances were not able to be explored in this study, given that, at baseline, 62.39 % of youth AFAB had already begun to experience pubertal development, a proportion consistent with, if slightly lower than, the ABCD baseline sample as a whole (Herting et al., 2021).

The only difference between the results for sex and pubertal status is that the variability of global efficiency was significantly related to sex, such that it was higher in those AFAB, while global efficiency variability was only borderline significantly related to a more advanced pubertal status. Although it may seem initially surprising that global efficiency, a measure of network integration, had the same direction of effect as the various measures of network segregation, it is important to note that functional integration across networks and functional segregation between networks are crucial developmental processes that occur simultaneously (Fair et al., 2007; 2009; Gracia-Tabuenca et al., 2021), so we do not necessarily expect that they work in opposition to each other. Additionally, regarding the lack of significance of global efficiency variability as it relates to pubertal status, previous work has demonstrated that local measures of network topology may be more temporally variable than global measures, and more reflective of changing network configurations (Chiang et al., 2016), and thus may be easier to detect. Due to the small number of

individuals at more advanced pubertal development (PDS categories 4 and 5), we may not have had enough power to detect changes related to puberty in global efficiency, particularly when accounting for the covariance between puberty and sex. If indeed the sex results do reflect an advanced maturation in those AFAB, the larger group size may have made the effect easier to detect. Additionally, although the PDS scale generally maps well onto biological measures of pubertal development, including at the hormonal level in ABCD (Herting et al., 2021), the PDS does have downsides, including being less informative at earlier pubertal stages (Dorn et al., 2006) and parent report being less useful than self-report at older ages (Cheng et al., 2021). Thus, our measure of puberty may be missing out on some relevant underlying source of variance. Alternatively, the effect of global efficiency may truly reflect a difference of sex that is completely separate from advanced pubertal or other maturation.

It is also notable that the variability of global efficiency decreased as a function of age, but as a function of sex, variability was higher in the AFAB group after controlling for the effect of age and, importantly, pubertal status. This finding is somewhat surprising if the effects of sex are indeed reflective of advanced maturation among youth AFAB. One potential explanation is that there are differential processes underlying the two effects. For example, the general decrease in global efficiency variability with age may be driven by the brain achieving a more modularized and functionally distinct state as children age (Fair et al., 2007; López-Vicente et al., 2021), while the increase in the variability of global efficiency, along with the metrics of segregation, in those AFAB may reflect increased switching between distinct functional states after accounting for this effect of age. Prior work has demonstrated that the development of distinct cognitive networks, particularly control networks, is a key characteristic of development (Fair et al., 2007, 2009), as is the ability to control the fluctuation of functional variability to flexibly move between states in response to situational demands (Hutchison and Morton, 2015). This more mature brain state, characterized by more defined, flexible networks and greater control of dynamically shifting between them, may be driven more by baseline differences in sex or pubertal development than by age directly, and this may be reflected as increased variability in those AFAB. Work in young adult samples has shown that those AFAB display a greater “stickiness” of brain states while those AMAB show an increased degree of brain dynamism (De Lacy et al., 2019), but it may be that those AFAB, or those more pubertally advanced, are reaching this stage of brain dynamism and exploration earlier and are further transitioning into a more stable state by adulthood. This is speculative, however, and importantly, past work in a similar age range (10–14 years) as the current work has actually demonstrated decreased state switching in those AFAB relative to those AMAB (López-Vicente et al., 2021). However, these functional states were defined very differently from the functional networks used in the present study, and thus may reflect a different process and cannot be compared directly to the current work. In general, further work is needed to compare the various commonly used measures of temporal dynamics (state-switching behavior as defined using *k*-means clustering, state-switching behavior defined using hidden (semi)-Markov models, graph theoretical metrics defined using rs-FC matrices, overall measures of temporal variability from rs-FC matrices, etc.) simultaneously and more

directly to better understand how they relate and index various types of fluctuations in rs-FC on different time scales (Cohen, 2018).

In general, it is somewhat surprising that the direction of the effects seen for age and pubertal maturation after accounting for the effect of age (e.g., increased variability in particular subnetworks as age increases, decreased variability in subnetwork connectivity as pubertal status advances) are opposing. As increased variability is commonly reported in the literature as individuals age and mature (López-Vicente et al., 2021; Marusak et al., 2017; Qin et al., 2015), this supports the idea that the age and pubertal maturation processes may be distinct, or at least that there is a (potentially quite large) effect of pubertal maturation on dynamic connectivity above and beyond the effect of age. Notably, the analyses for puberty control for the effect of age, and while there is a fairly narrow age band in the present sample, pubertal development during this age range is much more variable and may be less directly tied to age, allowing for more separation of their distinct effects. This idea is also broadly supported by the notable fact that there were many more significant findings for pubertal status (and sex) than for age in the present sample. This coheres with previous studies investigating the developmental trajectories of both age and puberty, which have found that models for pubertal development better describe developmental trajectories of brain development, and functional connectivity in particular, than models of age (Gracia-Tabuenca et al., 2021; Van Duijvenvoorde et al., 2019). This suggests that age may be a less precise or meaningful measure of maturation than pubertal status, which may more directly index ongoing developmental processes. The exact mechanisms underlying the effects of puberty on the brain remain somewhat unclear, but several potential mechanisms have been outlined for pubertal hormone-specific changes in brain structure such as cell proliferation, programmed cell death, and synaptic development and pruning that are supported by animal research, as reviewed by Goddings et al. (2019), as well as changes in brain function related to brain androgen and estrogen receptors. Although extrapolating findings from animal models to humans is not necessarily straightforward, particularly given the complex set of psychosocial, cultural, and environmental changes that accompany puberty in human adolescents, a limited body of research has directly related changes in pubertal hormone concentrations to changes in brain structure and function (Herting et al., 2014; Klapwijk et al., 2013; Peters et al., 2015; Spielberg et al., 2015). The effects of age and pubertal status are likely to be both distinct and overlapping, but also nonlinear and complex (Goddings et al., 2014, 2019; Wierenga et al., 2018), and future research is needed to carefully and rigorously disentangle the effects of each aspect of development. Additionally, given the body of evidence relating alterations in pubertal timing to various psychiatric disorders (Hayward, 2003), and our intentional selection of networks implicated in psychopathology for use in the current study, the particular networks under study here may be particularly likely to demonstrate changes related to pubertal development as opposed to age.

Finally, it is also interesting that within each aim or predictor group (e.g., looking at the effect of age controlling for sex and pubertal status, looking at the effect of sex controlling for the others, etc.), the direction of the effects of graph metric variability and within- and between-network variability were always opposing. For example, in the present analyses, we found that increased variability in graph metrics was always simultaneously associated with decreased variability in network connectivity. We found this pattern when evaluating

within-person associations as well. As the simultaneous investigation of these two metrics is rarely reported in the literature, it is not clear whether this is a property of the present developmental sample, or whether the two metrics should always be opposing and are measuring two different ends of an underlying phenomenon. Future research in this area should help elucidate this, and lead to a better understanding of what conclusions can be drawn from each metric.

The present study had several limitations that must be noted. First, the large sample size of the overall ABCD Study was significantly reduced in the current work, due to imaging data availability and the extremely strict motion criteria we implemented. To avoid using a large degree of motion censoring with the DCC method, due to the uncertain effects of linear interpolation on the results, we wanted to maximize subject availability while minimizing the amount of necessary interpolation. Thus we limited our sample to participants who had <10 frames above the motion threshold (i.e., <10 frames subject to linear interpolation). Further investigation into the effects of interpolation on DCC, and other dynamic FC analyses, should be conducted, and may allow us to substantially increase our sample size in the future. This strict motion criteria, although beneficial due to the numerous potential issues that motion can introduce in FC analyses, particularly in developmental samples (Satterthwaite et al., 2012, 2013), also raises the question of whether the remaining participants are biased in some way relative to the full sample. Indeed, we find that the included sub-sample is slightly older than the full sample, as well as lower in internalizing, ADHD and depression (at baseline) scores (Table S7). Although these differences are significant, they are relatively small in magnitude (e.g., maximum T-score differences of <1 point, a maximum age difference of about 1 month). Whether these differences in the sample are large enough to meaningfully change the conclusions we can draw is unclear.

Additionally, due to this strict motion criteria, and our desire to maximize the number of participants included, we included participants who had only one of the two time points (i.e., either baseline or year 2), rather than requiring all participants to have data available from both time points. As such, a more direct investigation of within-person change in the study was not implemented, but should be a direction for future research. Finally, recent work has highlighted that particular characteristics are associated with attrition in the ABCD sample (Feldstein Ewing et al., 2022) that may make the year 2 data somewhat less representative than the baseline data and introduce minor bias. Given how restricted the sample already is due to the strict motion criteria and limited availability of imaging data for some subjects, however, this is likely less of a concern than other potential sources of bias.

Another limitation of the present study is the difficulty in separating out the effects of sex and pubertal status, due the structure of the sample at this age range. As previously mentioned, nearly all individuals at the higher end of the PDS scale used to measure pubertal status are AFAB. As the ABCD Study progresses, and imaging data from later time points becomes available, the discrepancy in PDS category by sex should decrease, and disentangling the effects of pubertal development and sex should become easier. Additionally, although the PDS category is generally a good measure of biological pubertal development, and this has been validated in ABCD in particular (Herting et al., 2021), the PDS is really a measure of perceived pubertal stage and is not measuring pubertal

development directly, and as such has some limitations in measurement, particularly at earlier pubertal stages (Cheng et al., 2021; Dorn et al., 2006). Additionally, like all self-report and parent-report measures, the PDS is subject to potential inaccuracies, such as recall bias. Further, there is evidence that parent-reported PDS is less accurate at older ages but more accurate at younger ages (Cheng et al., 2021). Given that the majority of scans in the present sample are within this younger age range, in which the use of parent-reported PDS scores is explicitly recommended within the ABCD Study (Cheng et al., 2021), we elected to use only parent-report for consistency. Future work, however, may benefit from approaches that combine multiple measures of pubertal development (e.g., Herting et al., 2021) or a specification curve analysis approach that models the utilizes several different operationalizations of pubertal development (Cheng et al., 2021).

The present study uses the Glasser atlas, an atlas defined on adult samples. We selected the Glasser atlas due to its popularity in the imaging literature (e.g., Ito et al., 2017; Mansour et al., 2023; Zhao et al., 2023), including ABCD (e.g., Busch et al., 2024; Tomasi and Volkow, 2024) and other pediatric populations (e.g., Sydnor et al., 2023). Ideally, we would have used an atlas defined on a child sample, to avoid the potential confounding issue that increased coherence with the functional networks as children develop may affect the within- and between-network correlation values and subsequent metrics. However, well-defined functional whole-brain atlases derived specifically from age-appropriate pediatric samples have not been developed, and although promising work is beginning on developing structurally-defined atlases (Li et al., 2023), still-limited adoption constrains interpretations and comparisons to past work one can make with them. As such, we elected to use the Glasser atlas, but hope future work will fill this gap. Further, we elected to focus only on regions from core neurocognitive networks of particular interest during child and adolescent development and that have been related to psychopathology (FL, DMN, VCTC, DCTC), rather than all regions of the brain. Thus, we do not draw conclusions about whole brain variability in this age range, and sensory networks such as the somatomotor also show remarkable change during development (Uddin, 2010) that may potentially have different patterns. Future work should investigate a larger number of networks and whole-brain activity broadly. Additionally, although these specific networks were selected due to the importance of well-characterizing networks related to psychopathology for understanding how deviations in these metrics may relate to subsequent development of psychopathology, associations with psychopathology were not explicitly investigated in the current work, in part due to the relatively low incidence of a wide range of psychiatric disorders in this age range (Duffy et al., 2023). As the sample continues to develop into adolescence and as the incidence of clinical disorders increases toward expected levels, the relationship between dynamic variability and various indicators of psychopathology should be investigated.

Finally, we acknowledge the important difference between sex assigned at birth and gender identity, and importantly, that the two may have differential effects on the brain (Dhamala et al., 2024). We elected to focus here on sex assigned at birth, rather than gender identity, due to our interest in the effect of pubertal development, which differs greatly by sex in this age range (Patton and Viner, 2007). Further, there is a somewhat limited incidence of gender identities that do not cohere with sex assigned at birth in ABCD at this age (Papke, 2024). As imaging data for future time points becomes available and the incidence of those

identifying as a gender minority increases within the sample, the distinction between sex assigned at birth and gender identity should be thoroughly investigated, and is a particularly interesting avenue for future research given growing evidence for the hypothesis that the stress experienced by minoritized populations may contribute to early or advanced pubertal maturation (Argabright et al., 2022; Charlton et al., 2022).

Despite these limitations, the present study also had numerous advantages, including the use of a large, population-based sample designed to reflect the characteristics of US children overall and the use of a nonparametric model that does not assume linearity of effects over the course of development, as such linear effects are unlikely to exist (Vijayakumar et al., 2018; Zuo et al., 2017), particularly for the effects of sex and pubertal development (Gracia-Tabuenca et al., 2021; Vijayakumar et al., 2018). Overall, we feel this investigation into dynamic variability in the ABCD sample, and how it relates to age, sex, and pubertal development, opens the door to many interesting avenues for future research. Through a novel exploration of the variability of graph metrics and within- and between-network FC, we found that age was associated with increased variability within the fronto-limbic network, as well as for several other networks specifically for those AFAB, and we found that both advanced pubertal status and being AFAB were associated with increased variability in graph metrics indexing functional segregation and integration and decreased variability overall and within and between all networks under study. Our speculation that these results are potentially indicative of advanced maturation in those AFAB should be further investigated as more data from ABCD, and other large-scale imaging studies and consortia, become available. The congruence of results from other types of dynamic FC analyses, such as hidden (semi-) Markov models, in ABCD should also be investigated with the aim of moving the field towards a better understanding of the role dynamic activity and temporal variability play in childhood and adolescent development. This understanding will be critical to guide the understanding of the neurobiological basis of the emergence of psychopathology during this important developmental period.

Supplementary Material

Refer to Web version on PubMed Central for supplementary material.

Acknowledgements

The authors would like to thank the children, adolescents, and family members who participated in the study. This project was supported by NIH grants R01MH122473 for authors K.A.D., D.R., E.I., B.A.M., M.L., B. K-D., K.R.C, M.B.F. Author A.W. is funded by the National Science Foundation Graduate Research Fellowship Program. The authors would like to thank the Minnesota Supercomputing Institute (MSI) at the University of Minnesota for providing computing resources that were essential to conducting the research reported in this manuscript. Data used in the preparation of this article were obtained from the Adolescent Brain Cognitive Development (ABCD) Study (https://abcdstudy.org), held in the NIMH Data Archive (NDA). This is a multisite, longitudinal study designed to recruit >10,000 children age 9–10 and follow them over 10 years into early adulthood. The ABCD Study® is supported by the National Institutes of Health and additional federal partners under award numbers U01DA041048, U01DA050989, U01DA051016, U01DA041022, U01DA051018, U01DA051037, U01DA050987, U01DA041174, U01DA041106, U01DA041117, U01DA041028, U01DA041134, U01DA050988, U01DA051039, U01DA041156, U01DA041025, U01DA041120, U01DA051038, U01DA041148, U01DA041093, U01DA041089, U24DA041123, U24DA041147. A full list of supporters is available at https://abcdstudy.org/federal-partners.html. A listing of participating sites and a complete listing of the study investigators can be found at https://abcdstudy.org/consortium_members/. ABCD consortium investigators designed and implemented the study and/or provided data but did not necessarily participate in the analysis or writing of this report. This manuscript reflects the views of

the authors and may not reflect the opinions or views of the NIH or ABCD consortium investigators. The ABCD data repository grows and changes over time. The demographic ABCD data used in this report came from Data Release Version 5.1. For the imaging data, the raw DICOM data were downloaded from the ABCD FastTrack release and then processed using version 0.1.3 of the ABCD-BIDS pipeline from the Developmental Cognition and Neuroimaging (DCAN) Lab at the University of Minnesota. Further information on this pipeline can be found at https://github.com/DCAN-Labs/abcd-hcp-pipeline.

Data availability

In accordance with the Data Use Agreement, the asuthors are not able to directly share the Adolescent Brain Cognitive Development (ABCD) Study data used in this study. Eligible researchers who are interested in accessing the ABCD data themselves can request access to the ABCD Study under their own Data Use Agreement/Certification. Further information can be found at the ABCD Wiki (under FAQs: https://wiki.abcdstudy.org/faq/faq.html) and through the NDA (https://nda.nih.gov/user/dashboard/data_permissions.html). The authors are happy to share all code used in the present analyses to researchers with ABCD access to replicate all analysis steps.

References

Alarcón G, Cservenka A, Rudolph MD, Fair DA, Nagel BJ, 2015. Developmental sex differences in resting state functional connectivity of amygdala sub-regions. Neuroimage 115, 235–244. 10.1016/j.neuroimage.2015.04.013. [PubMed: 25887261]

Angold A, Costello EJ, 2006. Puberty and depression. Child Adolesc. Psychiatr. Clin. N. Am. 15 (4), 919–937. 10.1016/j.chc.2006.05.013.

Argabright ST, Moore TM, Visoki E, DiDomenico GE, Taylor JH, Barzilay R, 2022. Association between racial/ethnic discrimination and pubertal development in early adolescence. Psychoneuroendocrinology 140, 105727. 10.1016/j.psyneuen.2022.105727.

Auchter AM, Hernandez Mejia M, Heyser CJ, Shilling PD, Jernigan TL, Brown SA, Tapert SF, Dowling GJ, 2018. A description of the ABCD organizational structure and communication framework. Dev. Cogn. Neurosci. 32, 8–15. 10.1016/j.dcn.2018.04.003. [PubMed: 29706313]

Barucci E, Reno R, 2002. On measuring volatility and the GARCH forecasting ` performance. J. Int. Financ. Mark. Institut. Money 12 (3), 183–200. 10.1016/S1042-4431(02)00002-1.

Bates D, Maechler M, Bolker aut, cre B, Walker S, Christensen RHB, Singmann H, Dai B, Scheipl F, Grothendieck G, Green P, Fox J, Bauer A, simulate. formula), P NK (shared copyright on, Tansaka E, & Jagan M. (2024). lme4: linear mixed-effects models using “Eigen” and S4 (Version 1.1–35.3) [Computer software]. https://cran.r-project.org/web/packages/lme4/index.html.

Benjamini Y, Hochberg Y, 1995. Controlling the false discovery rate: a practical and powerful approach to multiple testing. J. R. Statist. Soc. 57 (1), 289–300. 10.1111/j.2517-6161.1995.tb02031.x.

Bollerslev T, 1986. Generalized autoregressive conditional heteroskedasticity. J. Econom. 31 (3), 307–327. 10.1016/0304-4076(86)90063-1.

Bullmore ET, Bassett DS, 2011. Brain graphs: graphical models of the Human Brain connectome. Annu Rev. Clin. Psychol. 7 (1), 113–140. 10.1146/annurev-clinpsy-040510-143934. [PubMed: 21128784]

Busch EL, Rapuano KM, Anderson KM, Rosenberg MD, Watts R, Casey BJ, Haxby JV, Feilong M, 2024. Dissociation of reliability, heritability, and predictivity in coarse- and fine-scale functional connectomes during development. J. Neurosci. 44 (6), e0735232023. 10.1523/JNEUROSCI.0735-23.2023.

Calhoun VD, Miller R, Pearlson G, Adalı T, 2014. The chronnectome: time-varying connectivity networks as the next frontier in fMRI data discovery. Neuron 84 (2), 262–274. [PubMed: 25374354]

Casey BJ, 2015. Beyond simple models of self-control to circuit-based accounts of adolescent behavior. Annu. Rev. Psychol. 66 (1), 295–319. 10.1146/annurev-psych-010814-015156. [PubMed: 25089362]

Casey BJ, Cannonier T, Conley MI, Cohen AO, Barch DM, Heitzeg MM, Soules ME, Teslovich T, Dellarco DV, Garavan H, Orr CA, Wager TD, Banich MT, Speer NK, Sutherland MT, Riedel MC, Dick AS, Bjork JM, Thomas KM, Dale AM, 2018. The Adolescent Brain Cognitive Development (ABCD) study: imaging acquisition across 21 sites. Dev. Cogn. Neurosci. 32, 43–54. 10.1016/j.dcn.2018.03.001. [PubMed: 29567376]

Chang C, Glover GH, 2010. Time–frequency dynamics of resting-state brain connectivity measured with fMRI. Neuroimage 50 (1), 81–98. 10.1016/j.neuroimage.2009.12.011. [PubMed: 20006716]

Charlton BM, Carwile JL, Chavarro JE, DiVasta AD, Ziyadeh NJ, Austin SB, 2022. Sexual orientation and age at menarche in three U.S. Longitudinal cohorts. J. Adolesc. Health 70 (1), 163–166. 10.1016/j.jadohealth.2021.06.029. [PubMed: 34404608]

Cheng TW, Magis-Weinberg L, Guazzelli Williamson V, Ladouceur CD, Whittle SL, Herting MM, Uban KA, Byrne ML, Barendse MEA, Shirtcliff EA, Pfeifer JH, 2021. A researcher's guide to the measurement and modeling of puberty in the ABCD study® at Baseline. Front. Endocrinol. 12, 608575. 10.3389/fendo.2021.608575.

Chiang S, Cassese A, Guindani M, Vannucci M, Yeh HJ, Haneef Z, Stern JM, 2016. Time-dependence of graph theory metrics in functional connectivity analysis. Neuroimage 125, 601–615. 10.1016/j.neuroimage.2015.10.070. [PubMed: 26518632]

Chittedi KR, 2015. Financial crisis and contagion effects to Indian stock market: 'DCC–GARCH' analysis. Glob. Bus. Rev. 16 (1), 50–60. 10.1177/0972150914553507.

Choe AS, Nebel MB, Barber AD, Cohen JR, Xu Y, Pekar JJ, Caffo B, Lindquist MA, 2017a. Comparing test-retest reliability of dynamic functional connectivity methods. Neuroimage 158, 155–175. [PubMed: 28687517]

Choe AS, Nebel MB, Barber AD, Cohen JR, Xu Y, Pekar JJ, Caffo B, Lindquist MA, 2017b. Comparing test-retest reliability of dynamic functional connectivity methods. Neuroimage 158, 155–175. 10.1016/j.neuroimage.2017.07.005. [PubMed: 28687517]

Christiansen DM, McCarthy MM, Seeman MV, 2022. Where sex meets gender: how sex and gender come together to cause sex differences in mental illness. Front. Psychiatry 13, 856436. 10.3389/fpsyt.2022.856436.

Cicchetti D, Toth SL, 2006. Building bridges and crossing them: translational research in developmental psychopathology. Dev. Psychopathol. 18 (03). 10.1017/S0954579406060317.

Cicchetti D, Toth SL, 2009. The past achievements and future promises of developmental psychopathology: the coming of age of a discipline. J. Child Psychol. Psychiatry 50 (1–2), 16–25. 10.1111/j.1469-7610.2008.01979.x. [PubMed: 19175810]

Cohen JR, 2018. The behavioral and cognitive relevance of time-varying, dynamic changes in functional connectivity. Neuroimage 180 (Pt B), 515–525. [PubMed: 28942061]

Craske MG, Stein MB, Eley TC, Milad MR, Holmes A, Rapee RM, Wittchen HU, 2017. Anxiety disorders. Nat. Rev. Dis. Prim. 3 (1), 17024. 10.1038/nrdp.2017.24. [PubMed: 28470168]

Damaraju E, Allen EA, Belger A, Ford JM, McEwen S, Mathalon DH, Mueller BA, Pearlson GD, Potkin SG, Preda A, Turner JA, Vaidya JG, Van Erp TG, Calhoun VD, 2014. Dynamic functional connectivity analysis reveals transient states of dysconnectivity in schizophrenia. NeuroImage 5, 298–308. 10.1016/j.nicl.2014.07.003. [PubMed: 25161896]

De Lacy N, McCauley E, Kutz JN, Calhoun VD, 2019. Sex-related differences in intrinsic brain dynamism and their neurocognitive correlates. Neuroimage 202, 116116. 10.1016/j.neuroimage.2019.116116.

Dhamala E, Bassett DS, Yeo BT, Holmes AJ, 2024. Functional brain networks are associated with both sex and gender in children. Sci. Adv. 10 (28), eadn4202. 10.1126/sciadv.adn4202.

Dorn LD, Dahl RE, Woodward HR, Biro F, 2006. Defining the boundaries of early adolescence: a user's guide to assessing pubertal status and pubertal timing in research with adolescents. Appl. Dev. Sci. 10 (1), 30–56. 10.1207/s1532480xads1001_3.

Duffy KA, Gandhi R, Falke C, Wiglesworth A, Mueller BA, Fiecas MB, Klimes-Dougan B, Luciana M, Cullen KR, 2023. Psychiatric diagnoses and treatment in nine- to ten-year-old participants

in the ABCD study. JAACAP Open 1 (1), 36–47. 10.1016/j.jaacop.2023.03.001. [PubMed: 38405128]

Engle R, 2002. Dynamic conditional correlation: a simple class of multivariate generalized autoregressive conditional heteroskedasticity models. J. Bus. Econ. Stat. 20 (3), 339–350. 10.1198/073500102288618487.

Faghiri A, Stephen JM, Wang Y, Wilson TW, Calhoun VD, 2018. Changing brain connectivity dynamics: from early childhood to adulthood. Hum. Brain Mapp. 39 (3), 1108–1117. 10.1002/hbm.23896. [PubMed: 29205692]

Fair DA, Cohen AL, Power JD, Dosenbach NUF, Church JA, Miezin FM, Schlaggar BL, Petersen SE, 2009. Functional brain networks develop from a “local to distributed” organization. PLoS Comput. Biol. 5 (5), e1000381. 10.1371/journal.pcbi.1000381.

Fair DA, Dosenbach NUF, Church JA, Cohen AL, Brahmbhatt S, Miezin FM, Barch DM, Raichle ME, Petersen SE, Schlaggar BL, 2007. Development of distinct control networks through segregation and integration. Proc. Natl. Acad. Sci. 104 (33), 13507–13512. 10.1073/pnas.0705843104. [PubMed: 17679691]

Fair DA, Miranda-Dominguez O, Snyder AZ, Perrone A, Earl EA, Van AN, Koller JM, Feczko E, Tisdall MD, Van Der Kouwe A, Klein RL, Mirro AE, Hampton JM, Adeyemo B, Laumann TO, Gratton C, Greene DJ, Schlaggar BL, Hagler DJ, Dosenbach NUF, 2020. Correction of respiratory artifacts in MRI head motion estimates. Neuroimage 208, 116400. 10.1016/j.neuroimage.2019.116400.

Feczko E, Conan G, Marek S, Tervo-Clemmens B, Cordova M, Doyle O, Earl E, Perrone A, Sturgeon D, Klein R, Harman G, Kilamovich D, Hermosillo R, Miranda-Dominguez O, Adebimpe A, Bertolero M, Cieslak M, Covitz S, Hendrickson T, … Fair DA (2021). Adolescent Brain Cognitive Development (ABCD) community MRI collection and utilities. 10.1101/2021.07.09.451638.

Feldstein Ewing SW, Dash GF, Thompson WK, Reuter C, Diaz VG, Anokhin A, Chang L, Cottler LB, Dowling GJ, LeBlanc K, Zucker RA, Tapert SF, Brown SA, Garavan H, 2022. Measuring retention within the adolescent brain cognitive development (ABCD) study. Dev. Cogn. Neurosci. 54, 101081. 10.1016/j.dcn.2022.101081.

Furman DJ, Hamilton JP, Gotlib IH, 2011. Frontostriatal functional connectivity in major depressive disorder. Biol. Mood. Anxiety. Disord. 1 (1), 11. 10.1186/2045-5380-1-11. [PubMed: 22737995]

Garavan H, Bartsch H, Conway K, Decastro A, Goldstein RZ, Heeringa S, Jernigan T, Potter A, Thompson W, Zahs D, 2018. Recruiting the ABCD sample: design considerations and procedures. Dev. Cogn. Neurosci. 32, 16–22. 10.1016/j.dcn.2018.04.004. [PubMed: 29703560]

Glasser MF, Coalson TS, Robinson EC, Hacker CD, Harwell J, Yacoub E, Ugurbil K, Andersson J, Beckmann CF, Jenkinson M, Smith SM, Van Essen DC, 2016. A multi-modal parcellation of human cerebral cortex. Nature 536 (7615), 171–178. 10.1038/nature18933. [PubMed: 27437579]

Goddings A, Beltz A, Peper JS, Crone EA, Braams BR, 2019. Understanding the role of puberty in structural and functional development of the adolescent brain. J. Res. Adolesc. 29 (1), 32–53. 10.1111/jora.12408. [PubMed: 30869842]

Goddings A-L, Mills KL, Clasen LS, Giedd JN, Viner RM, Blakemore S-J, 2014. The influence of puberty on subcortical brain development. Neuroimage 88, 242–251. 10.1016/j.neuroimage.2013.09.073. [PubMed: 24121203]

Gracia-Tabuenca Z, Moreno MB, Barrios FA, Alcauter S, 2021. Development of the brain functional connectome follows puberty-dependent nonlinear trajectories. Neuroimage 229, 117769. 10.1016/j.neuroimage.2021.117769.

Gur RE, Gur RC, 2016. Sex differences in brain and behavior in adolescence: findings from the Philadelphia Neurodevelopmental Cohort. Neurosci. Biobehav. Rev. 70, 159–170. 10.1016/j.neubiorev.2016.07.035. [PubMed: 27498084]

Hagler DJ, Hatton SeanN, Cornejo MD, Makowski C, Fair DA, Dick AS, Sutherland MT, Casey BJ, Barch DM, Harms MP, Watts R, Bjork JM, Garavan HP, Hilmer L, Pung CJ, Sicat CS, Kuperman J, Bartsch H, Xue F, Dale AM, 2019. Image processing and analysis methods for the Adolescent Brain Cognitive Development Study. Neuroimage 202, 116091. 10.1016/j.neuroimage.2019.116091.

Haist F, & Jernigan TL (n.d.). Adolescent Brain Cognitive Development Study (ABCD)—Annual Release 5.1. 10.15154/Z563-ZD24.

Harrison BJ, Soriano-Mas C, Pujol J, Ortiz H, López-Solà M, Hernández-Ribas R, Deus J, Alonso P, Yücel M, Pantelis C, Menchon JM, Cardoner N, 2009. Altered corticostriatal functional connectivity in obsessive-compulsive disorder. Arch. Gen. Psychiatry 66 (11), 1189. 10.1001/archgenpsychiatry.2009.152. [PubMed: 19884607]

Hastie T, Tibshirani R, 1987. Generalized additive models: some applications. J. Am. Stat. Assoc. 82 (398), 371–386. 10.1080/01621459.1987.10478440.

Hayward C, Sanborn K, 2002. Puberty and the emergence of gender differences in psychopathology. J. Adolesc. Health 30 (4), 49–58. 10.1016/S1054-139X(02)00336-1. [PubMed: 11943575]

Gender Differences at Puberty, 2003. Cambridge University Press.

Herting MM, Gautam P, Spielberg JM, Kan E, Dahl RE, Sowell ER, 2014. The role of testosterone and estradiol in brain volume changes across adolescence: a longitudinal structural MRI study. Hum. Brain Mapp. 35 (11), 5633–5645. 10.1002/hbm.22575. [PubMed: 24977395]

Herting MM, Uban KA, Gonzalez MR, Baker FC, Kan EC, Thompson WK, Granger DA, Albaugh MD, Anokhin AP, Bagot KS, Banich MT, Barch DM, Baskin-Sommers A, Breslin FJ, Casey BJ, Chaarani B, Chang L, Clark DB, Cloak CC, Sowell ER, 2021. Correspondence between perceived pubertal development and hormone levels in 9–10 year-olds from the adolescent Brain Cognitive Development study. Front. Endocrinol. 11, 549928. 10.3389/fendo.2020.549928.

Hutchison RM, Morton JB, 2015. Tracking the Brain's functional coupling dynamics over development. J. Neurosci. 35 (17), 6849–6859. 10.1523/JNEUROSCI.4638-14.2015. [PubMed: 25926460]

Hutchison RM, Womelsdorf T, Allen EA, Bandettini PA, Calhoun VD, Corbetta M, Della Penna S, Duyn JH, Glover GH, Gonzalez-Castillo J, Handwerker DA, Keilholz S, Kiviniemi V, Leopold DA, De Pasquale F, Sporns O, Walter M, Chang C, 2013. Dynamic functional connectivity: promise, issues, and interpretations. Neuroimage 80, 360–378. 10.1016/j.neuroimage.2013.05.079. [PubMed: 23707587]

Insel C, Kastman EK, Glenn CR, Somerville LH, 2017. Development of corticostriatal connectivity constrains goal-directed behavior during adolescence. Nat. Commun. 8 (1), 1605. 10.1038/s41467-017-01369-8. [PubMed: 29184096]

Ito T, Kulkarni KR, Schultz DH, Mill RD, Chen RH, Solomyak LI, Cole MW, 2017. Cognitive task information is transferred between brain regions via resting-state network topology. Nat. Commun. 8 (1), 1027. 10.1038/s41467-017-01000-w. [PubMed: 29044112]

Kebets V, Favre P, Houenou J, Polosan M, Perroud N, Aubry J-M, Van De Ville D, Piguet C, 2021. Fronto-limbic neural variability as a transdiagnostic correlate of emotion dysregulation. Transl. Psychiatry 11 (1), 545. 10.1038/s41398-021-01666-3. [PubMed: 34675186]

Kessler RC, Berglund P, Demler O, Jin R, Merikangas KR, Walters EE, 2005. Lifetime prevalence and age-of-onset distributions of DSM-IV disorders in the National comorbidity Survey replication. Arch. Gen. Psychiatry 62 (6), 593. 10.1001/archpsyc.62.6.593. [PubMed: 15939837]

Klapwijk ET, Goddings A-L, Burnett Heyes S, Bird G, Viner RM, Blakemore S-J, 2013. Increased functional connectivity with puberty in the mentalising network involved in social emotion processing. Horm. Behav. 64 (2), 314–322. 10.1016/j.yhbeh.2013.03.012. [PubMed: 23998674]

Kuznetsova A, Brockhoff PB, Christensen RHB, 2017. lmerTest Package: tests in linear mixed effects models. J. Stat. Softw. 82 (13). 10.18637/jss.v082.i13.

Kuznetsova A, Brockhoff PB, Christensen RHB, Jensen SP, 2020. lmerTest: Tests in Linear Mixed Effects Models (Version 3.1–3) [Computer software]. https://cran.r-project.org/web/packages/lmerTest/index.html.

Laird NM, Ware JH, 1982. Random-effects models for longitudinal data. Biometrics 38 (4), 963. 10.2307/2529876. [PubMed: 7168798]

Latora V, Marchiori M, 2001. Efficient behavior of small-world networks. Phys. Rev. Lett. 87 (19), 198701. 10.1103/PhysRevLett.87.198701.

Li W, Fan L, Shi W, Lu Y, Li J, Luo N, Wang H, Chu C, Ma L, Song M, Li K, Cheng L, Cao L, Jiang T, 2023. Brainnetome atlas of preadolescent children based on anatomical connectivity profiles. Cereb. Cortex 33 (9), 5264–5275. 10.1093/cercor/bhac415. [PubMed: 36255322]

Lin X, Zhang D, 1999. Inference in generalized additive mixed models by using smoothing splines. J. R. Stat. Soc. Ser. B 61 (2), 381–400. 10.1111/1467-9868.00183.

Lindquist MA, Xu Y, Nebel MB, Caffo BS, 2014. Evaluating dynamic bivariate correlations in resting-state fMRI: a comparison study and a new approach. Neuroimage 101, 531–546. 10.1016/j.neuroimage.2014.06.052. [PubMed: 24993894]

López-Ojeda W, Hurley RA, 2021. Sexual dimorphism in brain development: influence on affective disorders. J. Neuropsychiatry Clin. Neurosci. 33 (2), 85–89. 10.1176/appi.neuropsych.20100269.A4.

López-Vicente M, Agcaoglu O, Pérez-Crespo L, Estévez-López F, Heredia-Genestar JM, Mulder RH, Flournoy JC, Van Duijvenvoorde ACK, Güroglu B, White T, Calhoun V, Tiemeier H, Muetzel RL, 2021. ˇ Developmental changes in dynamic functional connectivity from childhood into adolescence. Front. Syst. Neurosci. 15, 724805. 10.3389/fnsys.2021.724805.

Luciana M, 2013. Adolescent brain development in normality and psychopathology. Dev. Psychopathol. 25 (4pt2), 1325–1345. 10.1017/S0954579413000643. [PubMed: 24342843]

Lydon-Staley DM, Ciric R, Satterthwaite TD, Bassett DS, 2019. Evaluation of confound regression strategies for the mitigation of micromovement artifact in studies of dynamic resting-state functional connectivity and multilayer network modularity. Netw. Neurosci. 3 (2), 427–454. 10.1162/netn_a_00071. [PubMed: 30793090]

Mansour LS, Di Biase MA, Smith RE, Zalesky A, Seguin C, 2023. Connectomes for 40,000 UK Biobank participants: a multi-modal, multi-scale brain network resource. Neuroimage 283, 120407. 10.1016/j.neuroimage.2023.120407.

Marusak HA, Calhoun VD, Brown S, Crespo LM, Sala-Hamrick K, Gotlib IH, Thomason ME, 2017. Dynamic functional connectivity of neurocognitive networks in children. Hum. Brain Mapp. 38 (1), 97–108. 10.1002/hbm.23346. [PubMed: 27534733]

Newman MEJ, 2003. The structure and function of complex networks. SIAM Review 45 (2), 167–256. 10.1137/S003614450342480.

Nychka D, 1988. Bayesian confidence intervals for smoothing splines. J. Am. Stat. Assoc. 83 (404), 1134–1143. 10.1080/01621459.1988.10478711.

Papke V, 2024. Sexual and Gender Minority Stress: Preliminary Evidence of Advanced Pubertal Development in Early Adolescence. The University Digital Conservancy [Master's thesis, University of Minnesota]. https://hdl.handle.net/11299/261976.

Patton GC, Viner R, 2007. Pubertal transitions in health. Lancet 369 (9567), 1130–1139. 10.1016/S0140-6736(07)60366-3. [PubMed: 17398312]

Paus T, Keshavan M, Giedd JN, 2008. Why do many psychiatric disorders emerge during adolescence? Nat. Rev. Neurosci. 9 (12), 947–957. 10.1038/nrn2513. [PubMed: 19002191]

Peters S, Jolles DJ, Duijvenvoorde ACKV, Crone EA, Peper JS, 2015. The link between testosterone and amygdala–orbitofrontal cortex connectivity in adolescent alcohol use. Psychoneuroendocrinology 53, 117–126. 10.1016/j.psyneuen.2015.01.004. [PubMed: 25618591]

Petersen AC, Crockett L, Richards M, Boxer A, 1988. A self-report measure of pubertal status: reliability, validity, and initial norms. J. Youth. Adolesc. 17 (2), 117–133. 10.1007/BF01537962. [PubMed: 24277579]

Qin J, Chen S-G, Hu D, Zeng L-L, Fan Y-M, Chen X-P, Shen H, 2015. Predicting individual brain maturity using dynamic functional connectivity. Front. Hum. Neurosci. 9. 10.3389/fnhum.2015.00418.

R Core Team, 2024. R: A Language and Environment for Statistical Computing [Computer Software]. R Foundation for Statistical Computing. https://www.R-project.org/.

Raichle ME, 2015. The brain's default mode network. Annu Rev. Neurosci. 38 (1), 433–447. 10.1146/annurev-neuro-071013-014030. [PubMed: 25938726]

Raichle ME, MacLeod AM, Snyder AZ, Powers WJ, Gusnard DA, Shulman GL, 2001. A default mode of brain function. Proc. Natl. Acad. Sci. 98 (2), 676–682. 10.1073/pnas.98.2.676. [PubMed: 11209064]

Rashid B, Blanken LME, Muetzel RL, Miller R, Damaraju E, Arbabshirani MR, Erhardt EB, Verhulst FC, Van Der Lugt A, Jaddoe VWV, Tiemeier H, White T, Calhoun V, 2018. Connectivity dynamics

in typical development and its relationship to autistic traits and autism spectrum disorder. Hum. Brain Mapp. 39 (8), 3127–3142. 10.1002/hbm.24064. [PubMed: 29602272]

Rubinov M, Sporns O, 2010. Complex network measures of brain connectivity: uses and interpretations. Neuroimage 52 (3), 1059–1069. 10.1016/j.neuroimage.2009.10.003. [PubMed: 19819337]

Satterthwaite TD, Wolf DH, Loughead J, Ruparel K, Elliott MA, Hakonarson H, Gur RC, Gur RE, 2012. Impact of in-scanner head motion on multiple measures of functional connectivity: relevance for studies of neurodevelopment in youth. Neuroimage 60 (1), 623–632. 10.1016/j.neuroimage.2011.12.063. [PubMed: 22233733]

Satterthwaite TD, Wolf DH, Ruparel K, Erus G, Elliott MA, Eickhoff SB, Gennatas ED, Jackson C, Prabhakaran K, Smith A, Hakonarson H, Verma R, Davatzikos C, Gur RE, Gur RC, 2013. Heterogeneous impact of motion on fundamental patterns of developmental changes in functional connectivity during youth. Neuroimage 83, 45–57. 10.1016/j.neuroimage.2013.06.045. [PubMed: 23792981]

Satterthwaite TD, Wolf DH, Roalf DR, Ruparel K, Erus G, Vandekar S, Gennatas ED, Elliott MA, Smith A, Hakonarson H, Verma R, Davatzikos C, Gur RE, Gur RC, 2015. Linked sex differences in cognition and functional connectivity in youth. Cereb. Cortex 25 (9), 2383–2394. 10.1093/cercor/bhu036. [PubMed: 24646613]

Schulz KM, Molenda-Figueira HA, Sisk CL, 2009. Back to the future: the organizational–activational hypothesis adapted to puberty and adolescence. Horm. Behav. 55 (5), 597–604. 10.1016/j.yhbeh.2009.03.010. [PubMed: 19446076]

Schulz KM, Sisk CL, 2006. Pubertal hormones, the adolescent brain, and the maturation of social behaviors: lessons from the Syrian hamster. Mol. Cell Endocrinol. 254–255, 120–126. 10.1016/j.mce.2006.04.025.

Schulz KM, Sisk CL, 2016. The organizing actions of adolescent gonadal steroid hormones on brain and behavioral development. Neurosci. Biobehav. Rev. 70, 148–158. 10.1016/j.neubiorev.2016.07.036. [PubMed: 27497718]

Shirtcliff EA, Dahl RE, Pollak SD, 2009. Pubertal development: correspondence between hormonal and physical development. Child Dev. 80 (2), 327–337. 10.1111/j.1467-8624.2009.01263.x. [PubMed: 19466995]

Solé-Padulles C, Castro-Fornieles J, De La Serna E, Calvo R, Baeza I, Moya J, Lázaro L, Rosa M, Bargalló N, Sugranyes G, 2016. Intrinsic connectivity networks from childhood to late adolescence: effects of age and sex. Dev. Cogn. Neurosci. 17, 35–44. 10.1016/j.dcn.2015.11.004. [PubMed: 26657414]

Spielberg JM, Forbes EE, Ladouceur CD, Worthman CM, Olino TM, Ryan ND, Dahl RE, 2015. Pubertal testosterone influences threat-related amygdala–orbitofrontal cortex coupling. Soc. Cogn. Affect. Neurosci. 10 (3), 408–415. 10.1093/scan/nsu062. [PubMed: 24795438]

Sydnor VJ, Larsen B, Seidlitz J, Adebimpe A, Alexander-Bloch AF, Bassett DS, Bertolero MA, Cieslak M, Covitz S, Fan Y, Gur RE, Gur RC, Mackey AP, Moore TM, Roalf DR, Shinohara RT, Satterthwaite TD, 2023. Intrinsic activity development unfolds along a sensorimotor–association cortical axis in youth. Nat. Neurosci. 26 (4), 638–649. 10.1038/s41593-023-01282-y. [PubMed: 36973514]

Syed MF, Lindquist MA, Pillai JJ, Agarwal S, Gujar SK, Choe AS, Caffo B, Sair HI, 2017. Dynamic functional connectivity states between the dorsal and ventral sensorimotor networks revealed by Dynamic conditional correlation analysis of resting-State functional magnetic resonance imaging. Brain Connect. 7 (10), 635–642. 10.1089/brain.2017.0533. [PubMed: 28969437]

Thijssen S, Collins PF, Luciana M, 2020. Pubertal development mediates the association between family environment and brain structure and function in childhood. Dev. Psychopathol. 32 (2), 687–702. 10.1017/S0954579419000580. [PubMed: 31258099]

Tomasi D, Volkow ND, 2024. Associations between handedness and brain functional connectivity patterns in children. Nat. Commun. 15 (1), 2355. 10.1038/s41467-024-46690-1. [PubMed: 38491089]

Uddin LQ, 2010. Typical and atypical development of functional human brain networks: insights from resting-state fMRI. Front. Syst. Neurosci. 4. 10.3389/fnsys.2010.00021.

Van Duijvenvoorde ACK, Westhoff B, De Vos F, Wierenga LM, Crone EA, 2019. A three-wave longitudinal study of subcortical–cortical resting-state connectivity in adolescence: testing age- and puberty-related changes. Hum. Brain Mapp. 40 (13), 3769–3783. 10.1002/hbm.24630. [PubMed: 31099959]

Vijayakumar N, Op De Macks Z, Shirtcliff EA, Pfeifer JH, 2018. Puberty and the human brain: insights into adolescent development. Neurosci. Biobehav. Rev. 92, 417–436. 10.1016/j.neubiorev.2018.06.004. [PubMed: 29972766]

Volkow ND, Koob GF, Croyle RT, Bianchi DW, Gordon JA, Koroshetz WJ, Perez-Stable EJ, Riley WT, Bloch MH, Conway K, Deeds BG, Dowling GJ, Grant, Howlett KD, Matochik JA, Morgan GD, Murray MM, Noronha A, Spong CY, Weiss SRB, 2018. The conception of the ABCD study: from substance use to a broad NIH collaboration. Dev. Cogn. Neurosci. 32, 4–7. 10.1016/j.dcn.2017.10.002. [PubMed: 29051027]

Watts DJ, Strogatz SH, 1998. Collective dynamics of 'small-world' networks. Nature 393 (6684), 440–442. 10.1038/30918. [PubMed: 9623998]

Whitfield-Gabrieli S, Ford JM, 2012. Default mode network activity and connectivity in psychopathology. Annu Rev. Clin. Psychol. 8 (1), 49–76. 10.1146/annurev-clinpsy-032511-143049. [PubMed: 22224834]

Wierenga LM, Langen M, Oranje B, Durston S, 2014. Unique developmental trajectories of cortical thickness and surface area. Neuroimage 87, 120–126. 10.1016/j.neuroimage.2013.11.010. [PubMed: 24246495]

Wierenga LM, Sexton JA, Laake P, Giedd JN, Tamnes CK, 2018. the Pediatric Imaging, Neurocognition, and Genetics Study, A key characteristic of sex differences in the developing brain: Greater variability in brain structure of boys than girls. Cereb. Cortex 28 (8), 2741–2751. 10.1093/cercor/bhx154. [PubMed: 28981610]

Wiglesworth A, Fiecas MB, Xu M, Neher AT, Padilla L, Carosella KA, Roediger DJ, Mueller BA, Luciana M, Klimes-Dougan B, Cullen KR, 2023. Sex and age variations in the impact of puberty on cortical thickness and associations with internalizing symptoms and suicidal ideation in early adolescence. Dev. Cogn. Neurosci. 59, 101195. 10.1016/j.dcn.2022.101195.

Williams LM, 2017. Defining biotypes for depression and anxiety based on large-scale circuit dysfunction: a theoretical review of the evidence and future directions for clinical translation. Depress. Anxiety. 34 (1), 9–24. 10.1002/da.22556. [PubMed: 27653321]

Wood S, 2023. mgcv: Mixed GAM Computation Vehicle with Automatic Smoothness Estimation (Version 1.9–1) [Computer software]. https://cran.r-project.org/web/packages/mgcv/index.html.

Wood SN, 2013. On p-values for smooth components of an extended generalized additive model. Biometrika 100 (1), 221–228. 10.1093/biomet/ass048.

Wood S, Scheipl F, 2020. gamm4: Generalized Additive Mixed Models Using "mgcv" and "lme4" (Version 0.2–6) [Computer software]. https://cran.r-project.org/web/packages/gamm4/index.html.

Wu K, Taki Y, Sato K, Hashizume H, Sassa Y, Takeuchi H, Thyreau B, He Y, Evans AC, Li X, Kawashima R, Fukuda H, 2013. Topological organization of functional brain networks in healthy children: differences in relation to age, sex, and intelligence. PLoS. One 8 (2), e55347. 10.1371/journal.pone.0055347.

Yu Q, Du Y, Chen J, Sui J, Adali T, Pearlson GD, Calhoun VD, 2018. Application of graph theory to assess static and dynamic brain connectivity: approaches for building brain graphs. Proc. IEEE 106 (5), 886–906. 10.1109/JPROC.2018.2825200.

Zhang C, Cahill ND, Arbabshirani MR, White T, Baum SA, Michael AM, 2016. Sex and age effects of functional connectivity in early adulthood. Brain Connect. 6 (9), 700–713. 10.1089/brain.2016.0429. [PubMed: 27527561]

Zhang K, Chan L, 2009. Efficient factor GARCH models and factor-DCC models. Quant. Finance 9 (1), 71–91. 10.1080/14697680802039840.

Zhao B, Li T, Li Y, Fan Z, Xiong D, Wang X, Gao M, Smith SM, Zhu H, 2023. An atlas of trait associations with resting-state and task-evoked human brain functional organizations in the UK Biobank. Imaging Neurosci. 1, 1–23. 10.1162/imag_a_00015.

Zhong X, Pu W, Yao S, 2016. Functional alterations of fronto-limbic circuit and default mode network systems in first-episode, drug-naïve patients with major depressive disorder: a meta-analysis of

resting-state fMRI data. J. Affect. Disord. 206, 280–286. 10.1016/j.jad.2016.09.005. [PubMed: 27639862]

Zuo X-N, He Y, Betzel RF, Colcombe S, Sporns O, Milham MP, 2017. Human connectomics across the life span. Trends Cogn. Sci. 21 (1), 32–45. 10.1016/j.tics.2016.10.005. [PubMed: 27865786]

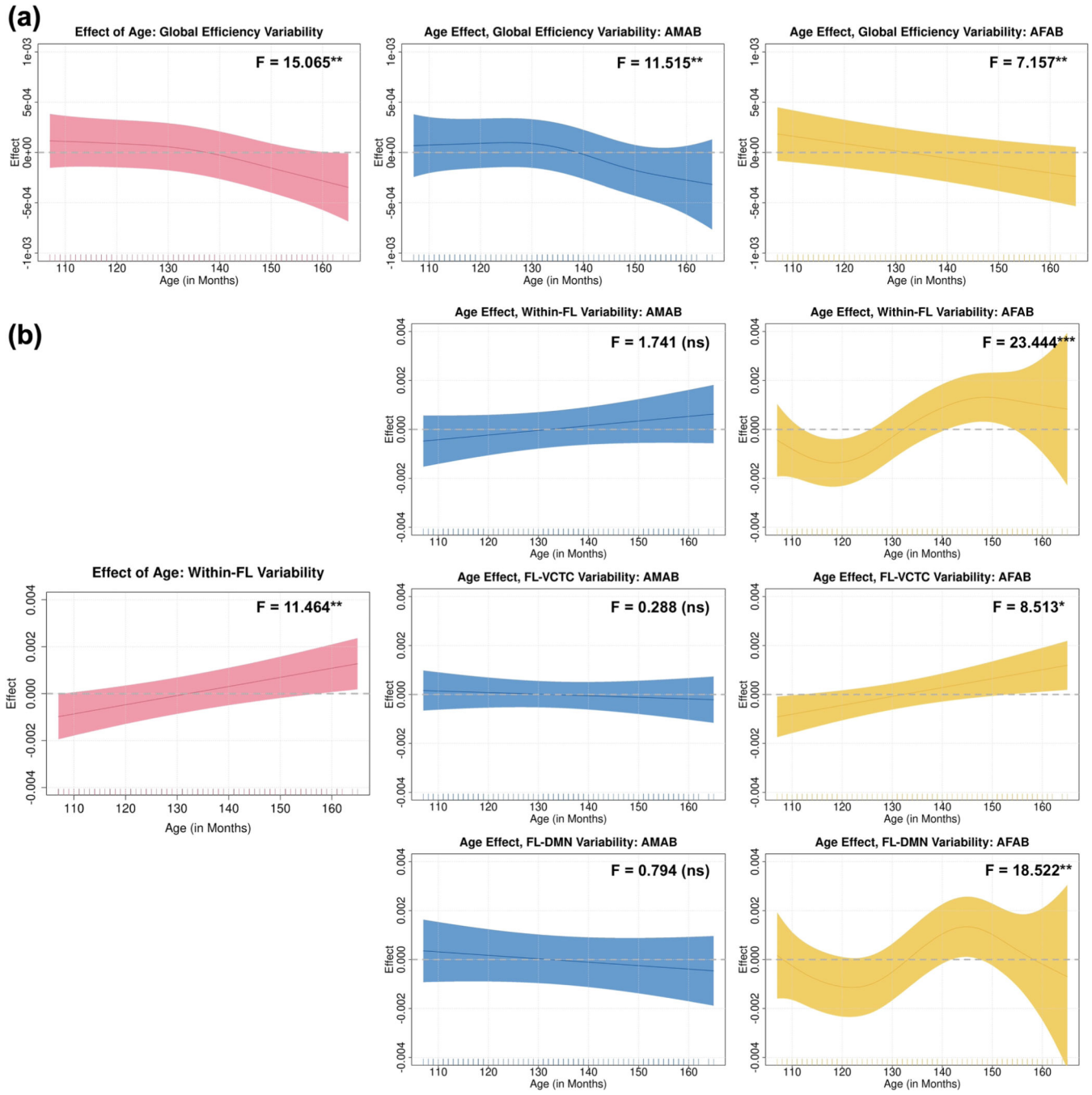

Fig. 1.

Smooth effect of age (in months), or the age–by-sex interaction, on the variability of graph metrics and within- and between-network correlations. Panel (a) shows the effect of age on the variability of global efficiency (left, pink coloring), the only graph metric to show a significant relationship with age. The age-by-sex interaction effect is also shown for the variability of global efficiency (the only graph metric to show significance) on the right. The center panel (with blue coloring) shows the effect of age on the variability of global efficiency for those assigned male at birth (AMAB). Right panel (yellow coloring) shows

the effect of age on the variability of global efficiency for those assigned female at birth (AFAB). Panel (b) shows the effect of age on the variability of within-frontolimbic (FL) connectivity (left, pink coloring), the only network to show a significant relationship with age. The smooth effect of the interaction between age (in months) and sex on the variability of within-frontolimbic (FL) connectivity, FL-ventral corticostriatal (VCTC) connectivity, and FL-DMN connectivity is shown on the right. Note that variability within several other networks (within-default mode [DMN], FL-dorsal corticostriatal [DCTC], FL-DMN, and DMN-VCTC connectivity, as well as the standard deviation (SD) of overall mean connectivity across the course of the scan [Mean SD]) also showed borderline significant age-by-sex interaction effects with a mean effect function very similar to that seen in FL-DMN connectivity, and each of these individual plots can be found in the Supplementary Materials. For each outcome, the center panel (with blue coloring) shows the effect of age for those assigned male at birth (AMAB), and the right panel (yellow coloring) shows the effect for those assigned female at birth (AFAB). For all plots, the solid dark line represents the mean effect, and shaded areas represent confidence bands of two standard errors around the smooth estimate. Note that confidence intervals account for the uncertainty around the mean, and as such, significant effects may show an overlap with 0 (indicated by the gray dashed line). Effects shown include pubertal status, sex (for the age-only effects), and demographic variables as covariates. Within each panel, the F test for the smooth effect is added as text in the top right, and the statistical significance of its corresponding (FDR-corrected) p-value is noted using asterisks, such that: *$p < .05$; **$p < .01$; ***$p < 0.001$. Plot made in part using package mgcv (Wood, 2023). (For interpretation of the references to color in this figure legend, the reader is referred to the web version of this article.)

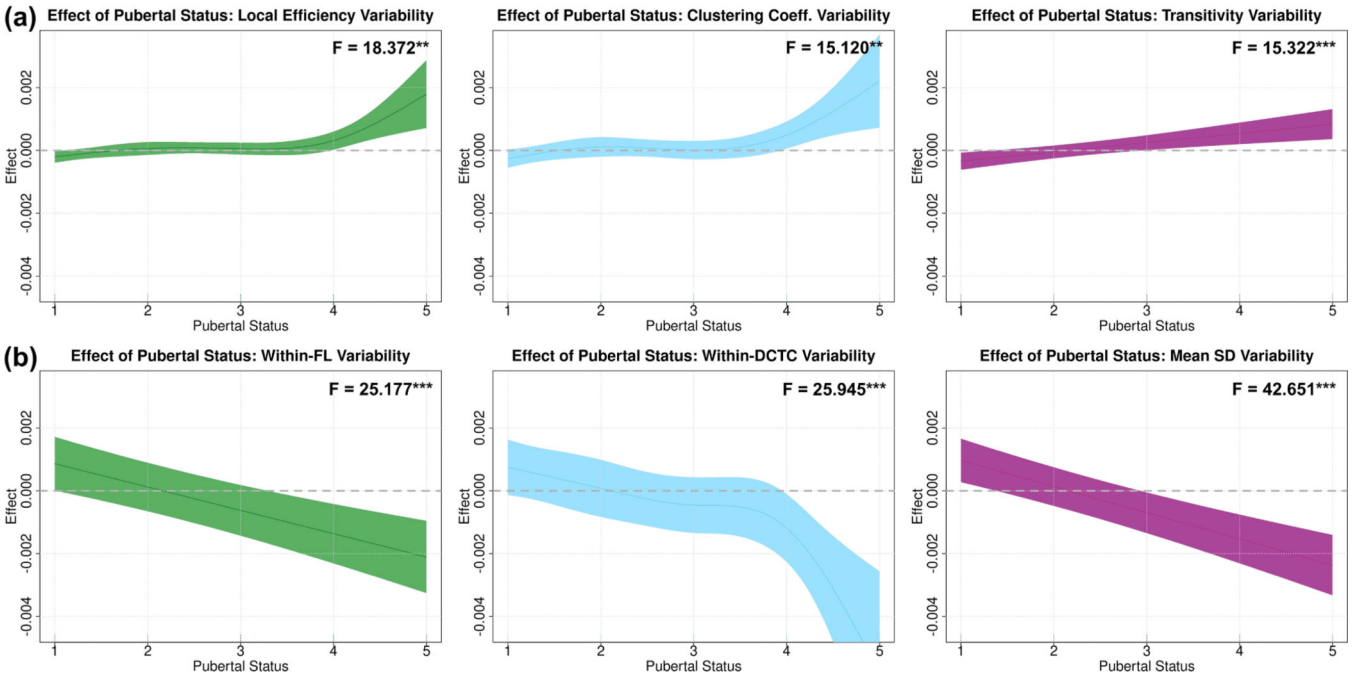

Fig. 2.

Smooth effect of pubertal status (measured as PDS categories 1 through 5) on the variability of graph metrics and within- and between-network connectivity. Panel (a), top row, shows the effect of PDS on all the variability of graph metrics that showed a significant relationship with pubertal status: local efficiency (left panel, green coloring), clustering coefficient (center panel, blue coloring), and transitivity (right panel, purple coloring). Panel (b), bottom row, shows the effect of PDS on the variability of within-frontolimbic (FL) connectivity (left panel, green coloring), within-dorsal corticostriatal (DCTC) connectivity (center panel, blue coloring), and the standard deviation (SD) of overall mean connectivity (Mean SD) across the course of the scan (right panel, purple coloring). Note that all within- and between-network pairs not shown here (within-default mode [DMN], within-ventral corticostriatal [VCTC], FL-DMN, FL-VCTC, FL-DCTC, DMN-VCTC, DMN-DCTC, VCTC-DCTC) also displayed significant effects of pubertal status, with mean effect functions that were extremely similar to those of within-FL and Mean SD; each of these individual plots can be found in the Supplementary Materials. For all plots, the solid dark line represents the mean effect, and shaded areas represent confidence bands of two standard errors around the smooth estimate. Note that confidence intervals account for the uncertainty around the mean, and as such, significant effects may show an overlap with 0 (indicated by the gray dashed line). Effects shown include age and demographic variables as covariates. Within each panel, the F test for the smooth effect is added as text in the top right, and the statistical significance of its corresponding (FDR-corrected) p-value is noted using asterisks, such that: *$p < .05$; **$p < .01$; ***$p < 0.001$. Plot made in part using package mgcv (Wood, 2023). (For interpretation of the references to color in this figure legend, the reader is referred to the web version of this article.)

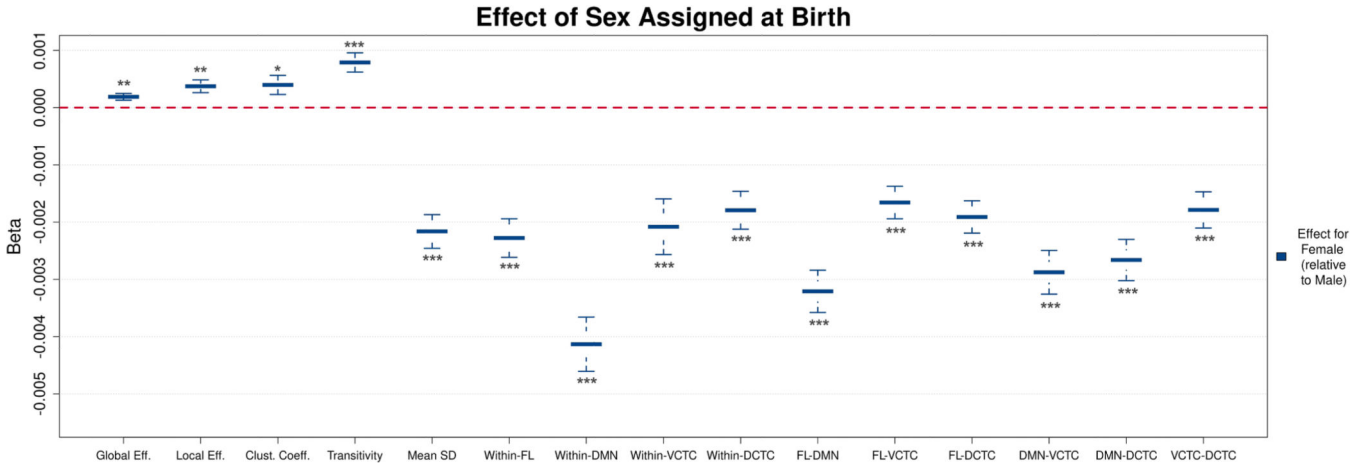

Fig. 3.

Effect of sex assigned at birth (measured as assigned male and assigned female) on the variability of all graph metrics and all within- and between-network connectivity values, as all outcomes showed a significant effect. Values represent the estimated coefficient (beta) for the effect of being assigned female at birth (blue lines), relative to being assigned male at birth (which always serves as the reference category), for the according outcome in the linear mixed effects model. Dashed lines represent the standard error of the estimated beta coefficient. All effects showed a significant relationship including age, pubertal status, and demographic variables as covariates. Asterisks represent significance cutoffs of the according (FDR-corrected) *p*-values, such that: *$p < .05$; **$p < .01$; ***$p < 0.001$. Network names are abbreviated as follows: frontolimbic (FL), default mode (DMN), ventral cortico-striatal (VCTC), and dorsal cortico-striatal (DCTC). (For interpretation of the references to color in this figure legend, the reader is referred to the web version of this article.)

Table 1

Demographic information for the overall sample of subjects included in the data, as well as the information for the unique subjects samples at Baseline and Year 2. Note that some subjects have data at both Baseline and Year 2, and data for both time points for these subjects is included in the "Overall" column, as some variables (e.g., age, pubertal status) vary across time points. Age (in years) is given as the sample average and standard deviation, while all other measures are given as the sample size (*n*) and corresponding percentage endorsing each category. Note that race and ethnicity is coded such that participants can identify as multiple categories; i.e., race and ethnicity categories are *not* mutually exclusive, and sample sizes and percentages thus do not add up to the sample total, but rather reflect the number and percentage of participants that endorsed that category in any way, potentially in addition to other categories. Also note that several variables were measured on more fine-grained scales, used in subsequent analyses, but have been coarsened here for presentation: household income was measured across 10 categories and coarsened, parental education was measured across 21 categories and coarsened (HS = High School), and age was measured in months but is presented in years.

	Overall	Baseline Only	Year 2 Only
N	5122	2594	2528
Age [mean (SD)]	11.02 (1.19)	10.03 (0.63)	12.05 (0.65)
Sex Assigned at Birth: Female (%)	2722 (53.1)	1396 (53.8)	1326 (52.5)
Pubertal Status (%)			
Pre-Puberty (1)	1793 (36.5)	1328 (52.8)	465 (19.4)
Early Puberty (2)	1109 (22.6)	578 (23.0)	531 (22.2)
Mid-Puberty (3)	1391 (28.3)	574 (22.8)	817 (34.1)
Late Puberty (4)	597 (12.2)	33 (1.3)	564 (23.5)
Post-Puberty (5)	22 (0.4)	2 (0.1)	20 (0.8)
Scanner Manufacturer (%)			
GE Medical Systems	937 (18.3)	596 (23.0)	341 (13.5)
Philips Medical Systems	246 (4.8)	44 (1.7)	202 (8.0)
Siemens	3939 (76.9)	1954 (75.3)	1985 (78.5)
Highest Caretaker Education (%)			
Some HS	152 (3.0)	75 (2.9)	77 (3.0)
HS Diploma	282 (5.5)	140 (5.4)	142 (5.6)
Assoc. Degree/Some College	1181 (23.1)	599 (23.1)	582 (23.0)
Bach. Degree	1525 (29.8)	770 (29.7)	755 (29.9)
Graduate Degree	1979 (38.7)	1008 (38.9)	971 (38.4)
Household/Combined Income (%)			
<$50k	952 (19.9)	534 (22.1)	418 (17.6)
$50–100k	1402 (29.3)	718 (29.7)	684 (28.8)
>$100k	2437 (50.9)	1165 (48.2)	1272 (53.6)
Race and Ethnicity (%)			
American Indian or Alaska Native	135 (2.6)	74 (2.9)	61 (2.4)
Asian	324 (6.3)	176 (6.8)	148 (5.9)
Black	754 (14.7)	366 (14.1)	388 (15.4)
Hispanic/Latinx	851 (16.8)	435 (17.0)	416 (16.6)

	Overall	Baseline Only	Year 2 Only
Missing	13 (0.3)	7 (0.3)	6 (0.2)
Native Hawaiian or Pacific Islander	38 (0.7)	20 (0.8)	18 (0.7)
Other	253 (4.9)	135 (5.2)	118 (4.7)
White	4218 (82.5)	2128 (82.2)	2090 (82.8)
Parental Marital Status (%)			
Divorced	454 (8.9)	231 (9.0)	223 (8.9)
Living with Partner	235 (4.6)	115 (4.5)	120 (4.8)
Married	3830 (75.2)	1937 (75.1)	1893 (75.3)
Never Married	386 (7.6)	203 (7.9)	183 (7.3)
Separated	160 (3.1)	83 (3.2)	77 (3.1)
Widowed	30 (0.6)	11 (0.4)	19 (0.8)